

Removal of Acid Yellow 25 Dye onto Chitin Extracted from Waste Crab legs and
Study of Adsorption Isotherms and Kinetics of AY25 Dye Adsorption

by Inoka Kumari Pathiraja, Bachelor of Science

A Thesis Submitted in Partial
Fulfillment of the Requirements
for the Degree of
Master of Science
in the field of Chemistry

Advisory Committee:

Chin-Chuan Wei, Chair

Leah O'Brien

Eric Voss

Graduate School
Southern Illinois University Edwardsville
August, 2014

UMI Number: 1565520

All rights reserved

INFORMATION TO ALL USERS

The quality of this reproduction is dependent upon the quality of the copy submitted.

In the unlikely event that the author did not send a complete manuscript and there are missing pages, these will be noted. Also, if material had to be removed, a note will indicate the deletion.



UMI 1565520

Published by ProQuest LLC (2014). Copyright in the Dissertation held by the Author.

Microform Edition © ProQuest LLC.

All rights reserved. This work is protected against unauthorized copying under Title 17, United States Code



ProQuest LLC.
789 East Eisenhower Parkway
P.O. Box 1346
Ann Arbor, MI 48106 - 1346

ABSTRACT

REMOVAL OF ACID YELLOW 25 DYE ONTO CHITIN EXTRACTED FROM WASTE CRAB LEGS AND STUDY OF ADSORPTION ISOTHERMS AND KINETICS OF ACID YELLOW 25 DYE ADSORPTION

by

INOKA KUMARI PATHIRAJA

Chairperson: Professor Chin-Chuan Wei

Acid Yellow 25 (AY25) is used in the textile industry for dyeing of natural fibers as well as synthetic fibers. To a lesser extent, it is also used as a coloring agent in paints, inks, plastics, and leather. Effluents from such industries are major sources of water pollution. Dyes in wastewater are difficult and costly to remove since they are stable to oxidizing agents and light. Hence, it is important to find simple, efficient, and inexpensive ways to remove the dyes from wastewater. The objective of this study is to determine the suitability of chitin extracted from waste crab legs as an adsorbent for removing AY25 dye. Purified chitin was characterized by Fourier transform infrared spectroscopy (FTIR) and X-ray powder diffraction methods. Batch adsorption experiments were performed to determine the effect of adsorbent dosage and initial dye concentration on percentage dye removal.

The adsorption kinetics were modeled using the pseudo-first order, pseudo-second order, and intra particle diffusion equations to determine the rate controlling step. Results showed that the pseudo-second order adsorption mechanism is predominant, and the overall rate of dye adsorption process is therefore controlled by adsorption reaction.

Adsorption data were analyzed using Langmuir, Freundlich, D-R and Temkin isotherm models at 23°C using various initial dye concentrations with different chitin dosages. Equilibrium data were fitted well with the Langmuir, Freundlich and D-R models giving the highest correlation with Langmuir model. This confirmed that chitin consists of both monolayer and homogeneous adsorption sites. Based on the D-R model, the adsorption of AY25 dye onto chitin was via chemisorption.

Same batch experiments were performed using unprocessed chitin and chitin extracted from red lobster shells to determine the efficiency of adsorption with different adsorbents. Results showed that unprocessed chitin is not a good adsorbent material. Chitin extracted from red lobster shell is better than that of crab legs giving the higher adsorptive capacity. In conclusion, chitin from waste crab legs is a very suitable adsorbent material that is capable of removing up to 95% of the initial concentration of AY25 dye. Also chitin is inexpensive and eco-friendly adsorbent found abundantly in nature.

ACKNOWLEDGEMENTS

I would like to express my deep gratitude to Dr. Chin-Chuan Wei for his priceless guidance and encouragement given to me during my research in last two years. I would also like to express my appreciation to him for giving me an opportunity to gain research experience as a volunteer student before I started my academic career at SIUE. His knowledge and motivation made me prepared not only for this research work but also for my entire future. I deeply appreciate Dr. Lawrence Norcio for his support and guidance for the success of my research work. My special thanks go to Dr. Leah O'Brien who always behind me, for giving me advice, knowledge and support whenever I needed and reviewing my thesis. I greatly appreciate Dr. Eric J. Voss for his guidance, support and knowledge given to me throughout my academic career at SIUE and reviewing my thesis. I would also like to acknowledge Dr. Luesse, Dr. Dixon, and Dr. Shabangi who made my knowledge broaden and made my journey at SIUE colorful and memorable.

I do want to thank the Department of Chemistry and the Graduate School at Southern Illinois University Edwardsville for offering me this opportunity to pursue my studies at SIUE. My sincere thanks also goes to laboratory Specialist and Lecturer, Mr. Brent Vaughn in Department of Civil Engineering at SIUE for providing sieves for my research work. I would like to thank all of my lab mates past and present specially Drake Jensen who helped me in many ways of my research during last two years.

Last but not least, I would like to thank my parents, family members, and my husband for all their support, keeping me motivated to work harder and sharing my sorrows and happiness throughout my life. They were always behind all my achievements and successes.

TABLE OF CONTENTS

ABSTRACT	ii
ACKNOWLEDGEMENTS	iv
LIST OF FIGURES	viii
LIST OF TABLES.....	ix
LIST OF EQUATIONS	x
LIST OF ABBREVIATIONS	xi
CHAPTER	
1 INTRODUCTION.....	1
1.1 Background.....	1
1.1.1 Usage of dyes in industry.....	1
1.1.2 Environmental and biological impacts of dyes.....	2
1.2 Acid Yellow 25 Dye (AY25).....	3
1.3 Methods of Dye Removal.....	3
1.3.1 Chemical methods.....	3
1.3.2 Biological methods.....	4
1.3.3 Physical methods.....	4
1.4 Selection of an Adsorbent for Dye Removal.....	5
1.5 Availability of Raw Material for Adsorbent.....	7
1.6 Chitin	8
1.6.1 Deacetylated chitin (chitosan).....	10
1.6.2 Degree of acetylation (DA) and degree of deacetylation (DD).....	10
1.7 Applications of Chitin and Chitosan.....	12
1.8 Adsorption.....	14
1.8.1 Dye adsorption mechanism	14
1.8.2 Adsorption kinetics.....	16
1.8.3 Adsorption isotherms	17
1.8.4 Types of adsorption	18
1.9 Merit of the Research.....	20

CHAPTER

2	REVIEW OF LITERATURE.....	21
2.1	Previous Research Related to Dye Removal	21
2.1.1	Tartrazine.....	22
2.1.2	Verofix red	22
2.1.3	Acid Yellow 25	23
2.1.4	Reactive dye Black 5 (RB5).....	23
2.1.5	Reactive Yellow 2 (RY2) and Reactive Black 5 (RB5).....	25

CHAPTER

3	EXPERIMENTAL.....	27
3.1	Extraction of Chitin.....	27
3.1.1	Preparation of raw materials.....	27
3.1.2	Demineralization	27
3.1.3	Deproteinization	28
3.1.4	Purification and sieving.....	28
3.2	Preparation of Chitosan.....	29
3.3	Characterization of Chitin/Chitosan	30
3.3.1	Fourier transform infrared spectroscopy (FTIR).....	30
3.3.2	X-ray powder diffractometry (XRD)	30
3.4	Adsorption Experiments	31
3.4.1	Batch treatment test.....	31
3.4.2	Adsorption isotherm test	32
3.4.3	Adsorption experiments using unprocessed chitin.....	33
3.4.4	Effect of the source of chitin	33
3.4.5	Statistical analysis	33

CHAPTER

4	RESULTS AND DISCUSSION.....	34
4.1	Extraction of Chitin.....	34
4.2	Characterization of Chitin.....	35
4.2.1	Fourier transform infrared spectroscopy	35
4.2.2	X-ray powder diffractometry (XRD)	37

4.3	Effect of Adsorbent Dosage on AY25 Dye Removal	39
4.4	Effect of Initial Dye Concentration on Adsorptive Capacity.....	40
4.4.1	Adsorptive capacity	40
4.5	Adsorption Kinetics	42
4.5.1	The pseudo-first order equation	43
4.5.2	The pseudo-second order equation.....	45
4.5.3	Intra particle diffusion model.....	48
4.6	Adsorption Isotherms.....	50
4.6.1	Adsorbent dosage method	51
4.6.2	Langmuir isotherm	52
4.6.2.1	Basic assumptions of the Langmuir model.....	55
4.6.3	Freundlich isotherm.....	56
4.6.3.1	Advantages of using Freundlich isotherm plots in adsorption studies.....	57
4.6.4	D-R (Dubinin–Radushkevich) isotherm model.....	59
4.6.5	Temkin isotherm model.....	62
4.7	Adsorption of AY25 Dye onto Unprocessed Chitin.....	64
4.8	Effect of Raw Material of Chitin	65
 CHAPTER		
5	CONCLUSION.....	67
REFERENCES		69

LIST OF FIGURES

Figure	Page
1. Chemical Structure of Acid Yellow 25 Dye	3
2. Comparison of % Dye Removal of Various Polysaccharide Adsorbents	6
3. Global Snow Crab Consumption in 2005	7
4. Global Snow Crab Suppliers from 1990 to 2005.....	7
5. The Amount of Snow Crab Imported to the United States during the period of 1990 to 2005	8
6. Chemical Structure of fully N-acetylated Chitin	9
7. Chemical Structure of Completely N-deacetylated Chitosan	10
8. Degrees of Acetylation and Deacetylation of Chitin and Chitosan	11
9. Three Steps (1,3 and 4) involved in Adsorption Mechanism	15
10. Types of Characteristic Isotherms	19
11. Scheme of the Extraction of Chitin from Crab Legs	29
12. ATR-FTIR Spectrophotometer	30
13. FT-IR Spectra of Chitin (A) and Chitosan (B) Extracted from Crab Legs, Chitin Extracted from Red Lobster Shells (C), β -chitin from Cuttlefish	35
14. XRD Pattern of Chitin Extracted from Crab Legs	37
15. Effect of Adsorbent Dosage on AY25 Dye Removal	39
16. Effect of Initial Dye Concentration on Adsorptive Capacity	41
17. Pseudo-first order Kinetic Model for AY25 Dye Adsorption onto Chitin	44
18. Pseudo-second order Kinetic Model for AY25 Dye Adsorption onto Chitin	46
19. Intra Particle Diffusion Model for AY25 Dye Adsorption onto Chitin	49
20. Effect of Chitin Dosage on Equilibrium Dye Concentration at 23°C and pH=2.....	51
21. Characteristic Shapes of Langmuir Saturation Curve (A) and Linearized Plot (B). 53	53
22. Langmuir Adsorption Isotherm Plots for the AY25 Dye Adsorption onto Chitin... 54	54
23. Freundlich Adsorption Isotherm Plots for the AY25 Dye Adsorption onto Chitin..58	58
24. D-R Adsorption Isotherm Plots for the AY25 Dye Adsorption onto Chitin	61
25. Temkin Adsorption Isotherm Plots for the AY25 Dye Adsorption onto Chitin.....63	63
26. Comparison of Dye Removal Capability of Chitin and Unprocessed Chitin at 23°C.....	64
27. Freundlich Adsorption Isotherm Plots for the AY25 Dye Adsorption onto Chitin..65	65

LIST OF TABLES

Table		Page
1.	Dye Loss to Effluent for Different Dye-fiber Systems	1
2.	Applications of Chitin, Chitosan and its Derivatives.....	13
3.	Kinetic Model Equations used for Dye Adsorption Process	17
4.	Equations of Adsorption Isotherm Models at Equilibrium.....	18
5.	Adsorptive Capacities of Different Adsorbents on Various Dyes	21
6.	Kinetic Parameters for Dye Adsorption onto Chitin.....	23
7.	Langmuir Isotherm Parameters for RB5 Adsorption onto Chitin	24
8.	Kinetic Parameters for RB5 Dye Adsorption onto Chitin.....	24
9.	Langmuir and Freundlich Isotherm Parameters for RB5 Dye Adsorption on to Chitin at different temperatures.....	25
10.	Kinetic Parameters related to the Adsorption of RY2 and RB5 onto Chitin.....	25
11.	Kinetic Parameters for AY25 Dye Adsorption onto Chitin	47
12.	Adsorptive Capacity Values at 95% Dye Removal in three Different Initial Dye Concentrations at 23°C according to the Adsorbent Dosage Method.....	52
13.	Langmuir Adsorption Isotherm Parameters for AY25 Dye Adsorption onto Chitin at 23°C.....	55
14.	Freundlich Adsorption Isotherm Parameters for AY25 Dye Adsorption onto Chitin and Adsorptive Capacities at 95% Dye Removal at 23°C	59
15.	D-R Isotherm Parameters and Mean free energy (E_{DR}) Values for AY25 Dye Adsorption onto Chitin at 23°C	61
16.	Temkin Adsorption Isotherm Parameters for AY25 Dye Adsorption onto Chitin at 23°C.....	64
17.	Freundlich Adsorption Isotherm Parameters for AY25 Dye Adsorption onto Chitin and Adsorptive Capacities at 95% Dye Removal at 23°C	66

LIST OF EQUATIONS

Equation	Page
1. Degree of Deacetylation	29
2. % Removal of Dye	31
3. Adsorptive Capacity at time t	32
4. Adsorptive Capacity at Equilibrium	40
5. Pseudo-first order Kinetic Equation	43
6. Integrated Pseudo-first order Kinetic Equation	43
7. Pseudo-second order Kinetic Equation	45
8. Integrated Pseudo-second order Kinetic Equation	45
9. Intra Particle Diffusion Equation	48
10. Langmuir Equation	52
11. Langmuir Equation after Rearranged	53
12. Equilibrium Parameter (Separation Factor)	53
13. Freundlich Isotherm	56
14. Linear form of Freundlich Isotherm	56
15. D-R Isotherm	59
16. Linear form of D-R Isotherm	59
17. Polyani Potential	60
18. Mean Free Energy	60
19. Temkin Isotherm	62
20. Linear form of Temkin Isotherm	63
21. Rate of Chitin Usage	66

LIST OF ABBREVIATIONS

AY25	:	Acid Yellow 25
BOD	:	Biological oxygen demand
SEM	:	Scanning electron microscopy
DA	:	Degree of acetylation
DD	:	Degree of deacetylation
FTIR	:	Fourier transform infrared spectroscopy
XRD	:	X-Ray powder diffractometry
rpm	:	Round per minute
SD	:	Standard deviation
BET	:	Brunauer–Emmett–Teller
D-R	:	Dubinin–Radushkevich

CHAPTER 1

INTRODUCTION

1.1 Background

1.1.1 Usage of dyes in industry

It was reported that annual worldwide dye production is about two million tons and 50% of those are azo dyes.¹ Azo dyes are a large class of synthetic dyes whose molecules contain two adjacent nitrogen atoms between carbon atoms. Dyes are extensively used in textile, plastic, leather, food, paper, paints, inks, cosmetics and pharmaceutical industries. The textile industry uses more than 10,000 different dyes in large quantities.¹ The overall average dye waste into the environment is 15% after dyeing.¹ Approximately 280,000 tons of textile dyes are let out into the environment worldwide per year and most of this ends up in the marine environment.² Table 1 summarizes the loss of dye into effluent after dyeing for different dye-fiber systems.

Table 1: Dye loss to effluent for different dye-fiber systems²

Dye class	Fiber	Loss to effluent (%)
Acid	Polyamide	5-20
Basic	Acrylic	0-5
Direct	Cotton	5-30
Disperse	Polyester	0-10
Metal-complex	Wool	2-10
Reactive	Cotton	10-50
Vat	Cotton	5-20

Acid dyes denote a large group of anionic dyes with a relatively low molecular weight that carry one to three sulfonic groups. They are mainly mono-azo compounds but also include diazo, nitro, 1-amino-anthraquinone, triphenyl methane, and other groups of compounds. The name “acid dye” is derived from the dyeing process; the dyes are applied to fibers in weakly acidic solution (pH 2 to 6).³

1.1.2 Environmental and biological impacts of dyes

Disposal of dyes into water streams is the major source of water pollution. Many dyes are visible in water at concentration as low as 1 mg/L. Textile processing waste waters typically contain 10-200 mg/L of dye.⁴

Dyes present in water streams affect photosynthesis by reducing light penetration, causing damage to the aquatic life. The textile dyes profoundly disturb the marine ecosystem as they undergo chemical and biological changes. In long term, their breakdown products might also be toxic to some aquatic organisms.⁵ However, as dyes are designed to be chemically and photolytically stable, they are highly persistent in natural environments. The release of dyes may therefore present an eco-toxic hazard and introduce the potential danger of bioaccumulation that may eventually affect human by transport through the food chain.⁴ Therefore, it needs to be removed before discharging into water bodies.

1.2 Acid Yellow 25 Dye (AY25)

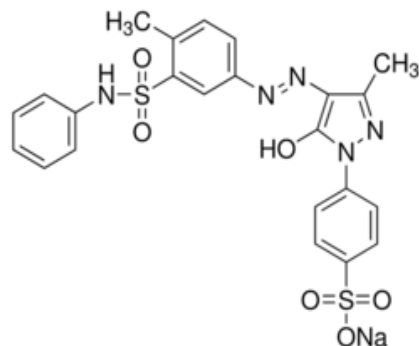


Figure 1: Chemical structure of Acid Yellow 25 dye⁶

Acid Yellow 25 dye ($C_{23}H_{20}N_5NaO_6S_2$) is a mono-azo acid dye with a molecular weight of 549.56 gmol^{-1} . It is highly intense in color even at very low concentration and its maximum light absorbance is observed at 392 nm. This dye is widely used in the textile industry for dyeing of natural fibers like cotton, wool and silk as well as synthetic fibers like polyesters, acrylic and rayon. To a lesser extent it is used as a coloring agent in paints, ink, plastics and leather industries.⁴

1.3 Methods of dye removal

The non-biodegradable nature of dyes and their stability toward light and oxidizing agents complicate the selection of a method for their removal. So far various chemical, biological and physical methods have been introduced and are discussed below.^{2,5}

1.3.1 Chemical methods

In chemical methods, the basic step in the decolorization and degradation of dyes is breakdown of azo bonds, leading to removal of color and toxicity of the dyes. Coagulation, electro-kinetic coagulation, flocculation combined with flotation, electro-flocculation,

electrochemical destruction, irradiation, precipitation, oxidation, ozonation, and katox treatment are some of the chemical methods that are currently used for dye removal.⁵ The major disadvantages of these methods are the high cost, low efficiency, limited versatility and utilize significant amount of energy used. Also these techniques generate a huge volume of sludge and cause secondary pollution, which creates environmental problems. Although the colors are removed by these processes due to the partial break down of the dye molecules, toxic derivatives such as primary aromatic amines and heavy metals may still exist in the treated liquor. Some electrochemical methods have been introduced that are highly effective with no chemical consumption, but the technology is relatively very expensive and hence not economically viable.⁵

1.3.2 Biological methods

The use of microorganisms for the removal of synthetic dyes offers considerable advantages; the process is relatively inexpensive, the running costs are low, and the degradation forms completely mineralized products.² However, these methods need large land area and are sensitive towards variants. Therefore, they are less flexible in design and operation. Also, some of the dyes are resistant to aerobic digestion. Biological treatments using activated sludge (bacterial oxidation) can reduce BOD (biological oxygen demand) but do not effectively remove color, as the oxidation rate is very slow.⁵

1.3.3 Physical methods

Filtration, ion-exchange, membrane filtration, and adsorption are some of the physical methods for dye removal. Membrane use in filtration has limited life time and hence is costly

to replace and is prone to pore clogging. The ion-exchange method is used to remove both cationic and anionic dyes. There is no loss of adsorbent on regeneration and the solvent is reclaimed after use. However, this method is not effective for all dyes, so it has not been widely used for the treatment of dye effluent.⁵ Adsorption is currently used for dye removal that involves the use of adsorbent. Adsorption removes the complete molecule, leaving no fragments in the wastewater and can be a very effective, low-cost method of color removal.¹

Even though many processes are available to clear up the color in textile waste water, none of the methods has yet proven itself on an industrial scale to provide a satisfactory solution. Among the above mentioned methods, adsorption is considered to be superior to other techniques because of low cost, simplicity of design, availability, easy to recover and the ability to treat dyes in a more concentrated form. Hence, adsorption is used in our study to provide a simple, efficient and cheap approach to remove Acid Yellow 25 dye.

1.4 Selection of an adsorbent for dye removal

Researchers investigated the feasibility of using various materials as adsorbent such as bentonite clay, bamboo dust, coconut shells, wheat bran, peat, wood, fly ash, and coal.⁷ Activated carbon has been widely studied and proven to have high adsorption capability to remove a large number of organic compounds.⁷ However, its use is limited mainly because of its high cost. Also, the performance is dependent on the type of carbon used, the characteristics of the waste water, and the type of dye.⁵ Other currently used adsorbents such as alum, polyaluminum chloride, and silica gel are not entirely eco-friendly themselves.⁷ So, the research of recent years mainly focused on utilizing natural materials as alternatives to activated carbon. Figure 2 shows the comparison of % dye removal capability of various polysaccharide adsorbents on three different dyes after 12 hours treatment.⁷

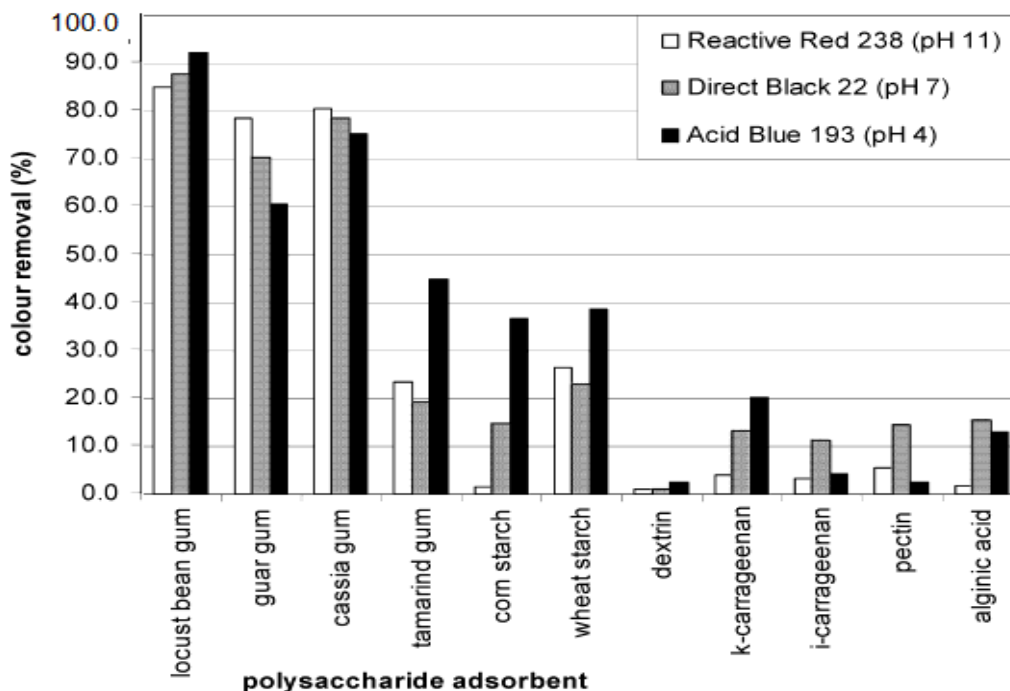


Figure 2. Comparison of % dye removal of various polysaccharide adsorbents⁷

Industry requires highly effective, low-cost adsorbents that are available in tonnage quantities and do not present an environmental problem. Therefore, there is still a need to develop cheap and effective adsorbents. In this study, chitin prepared from waste crab legs was used as an adsorbent to remove AY25 dye from aqueous solution. Chitin has been characterized as an excellent adsorbent due to its abundance, nontoxicity, biocompatibility, biodegradability, antibacterial property, inexpensiveness, and effective adsorptive ability. Interestingly, chitin has not been used in the removal of AY25. Our study presented the removal of the aqueous AY25 dye solution during chitin adsorption process.

1.5 Availability of raw material for adsorbent

In this study, waste snow crab legs were used to extract chitin. According to the statistics, the consumption of snow crabs in the United States is nearly 50,000 tons per year.⁸ The United States is the dominant market, taking about 70% of exports from the Atlantic snow crab industry. Figure 3 shows the global snow crab consumption in 2005. Figure 4 illustrates the global snow crab suppliers from 1990 to 2004.⁸

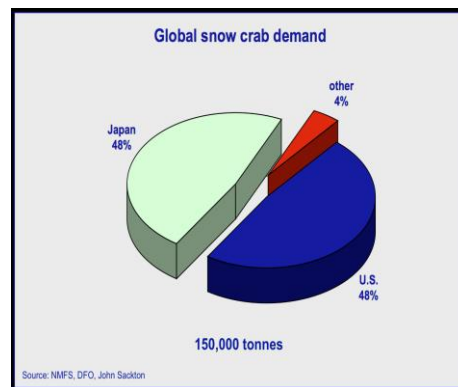


Figure 3: Global snow crab consumption in 2005 - The global market for snow crab is estimated at US\$ 670 million (export value). Two countries (U.S. and Japan) share about equally 96% of the market and total global snow crab consumption is 150,000 tons in 2005⁸

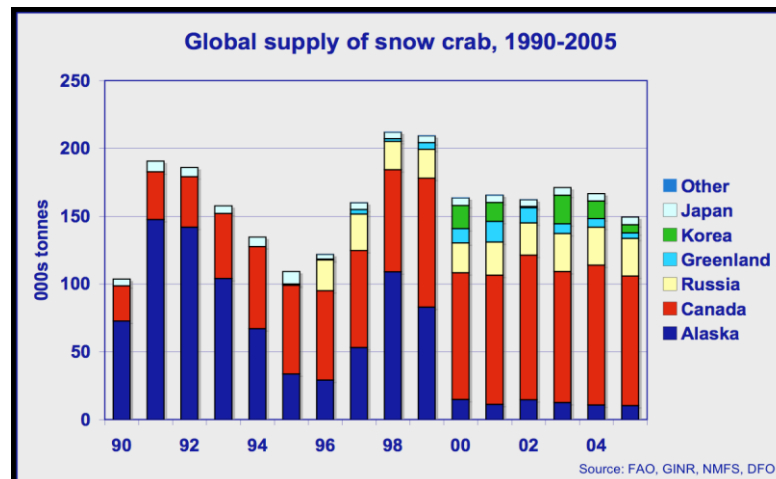


Figure 4: Global snow crab suppliers from 1990 to 2005 -Six countries produce the global supply of snow crab, estimated at 150-170,000 tons annually over the past five years. Canada is the leading producer, supplying over two-thirds.⁸

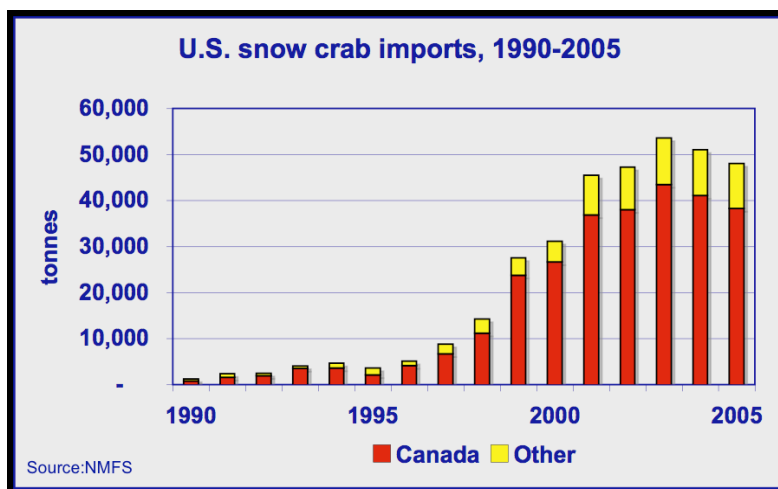


Figure 5: The amount of snow crab imported to the United States during the period of 1990 to 2005.⁸

According to these statistics, due to the large consumption of snow crabs in the United States, waste crab shell management has become another environmental issue.⁹ Even though there are several waste processing plants available throughout the country, they consume large amount of money, energy and labor. For example, it was reported that Maryland's Eastern Shore, one of the waste crab shell processing plants in the United States, processes up to 8 million pounds of waste crab shells per year.⁹

In our study, we used crab legs as the proposed raw material for chitin, this approach is an eco-friendly recycling method, as using one waste is clean up other waste. This crab-waste recycling method can also benefit the fishery and food industries by saving on their waste management expenses and reduce the effluent treatment cost to the textile industry.

1.6 Chitin

Chitin, next to cellulose, is the second most plentiful organic biopolymer on the Earth. It is found in plants, marine invertebrates, such as crabs, lobsters and shrimps, insects, cell walls of some fungi, and microorganisms. This polymer consists of long chain of

N-acetyl-D-glucosamine (NAG or 2-acetamido-2-deoxy-D-glucopyranose) units linked through β -1,4-glycosidic linkages. Naturally, chitin associates with proteins, organic pigments, and minerals.¹⁰ The content of chitin varies from one source to another. For example, crustacean shells contain primarily chitin with calcium carbonate, making the chitin polymer stronger and the mineral less brittle. In insect cuticles, it contains chitin with other structurally rigid proteins such as sclerotin and with colored pigments.¹⁰

Three different polymorphs of chitin are found in nature: α -, β -, and γ -chitin. α -chitin is the most common structure in nature, which corresponds to tightly compact orthorhombic cells formed by alternating sheets of antiparallel chains. This molecular arrangement is favorable for the formation of strong inter-molecular hydrogen bonding and therefore, α -chitin is the most stable form of three crystalline variations. β -chitin is a monoclinic unit cell structure where the polysaccharide chains are in parallel fashion, leading to weaker intermolecular forces. Thus, it is assumed to be less stable than α -chitin. γ -chitin is the least abundant polymorphs among the others and its structure has not been completely identified. It has been suggested that γ -chitin has a structure of combination of α and β rather than as a different polymorph.^{11,12}

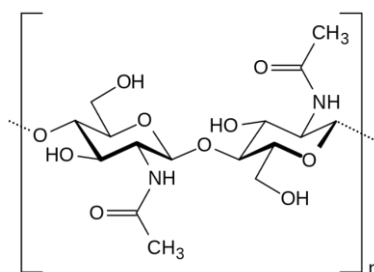


Figure 6: Chemical structure of fully N-acetylated Chitin¹³

α -chitin is usually extracted from the exoskeleton of crustaceans particularly from shrimps, lobsters and crabs. β -chitin can be obtained from squid pens while γ -chitin exists in fungi, stomach cuticles of cephalopoda and yeast.^{11,14} There is a significant difference in the

surface of α - and β -chitin: α -chitin has uniform and dense structure whereas β -chitin is less crystalline and is not uniform.¹⁵

1.6.1 Deacetylated Chitin (Chitosan)

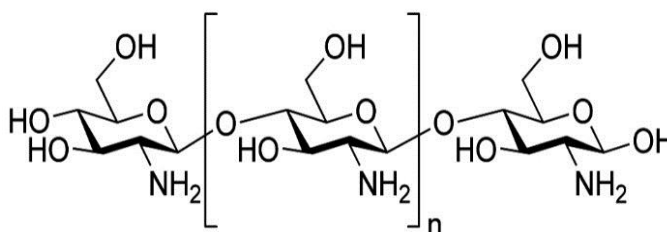


Figure 7: Chemical structure of completely N-deacetylated Chitosan¹⁶

The word “chitosan” is used for both partially and completely N-deacetylated chitin. Chitosan is a polymer of 2-amino-2-deoxy-D-glucose with β -1,4-glycosidic linkages. An important feature of chitosan is the degree of deacetylation.

1.6.2 Degree of Acetylation (DA) and Degree of Deacetylation (DD)

In fact, chitin and chitosan are not homopolysaccharides, in which their amine groups can be acetylated. The degree of N-acetylation (DA) has been employed to differentiate chitin from chitosan. Chitin is referred to a polymer when the DA is greater than 50% and the sample is not soluble; otherwise, it is called chitosan. Degree of deacetylation (DD) of chitosan has been found to influence its physical, chemical and biological activities.¹⁷

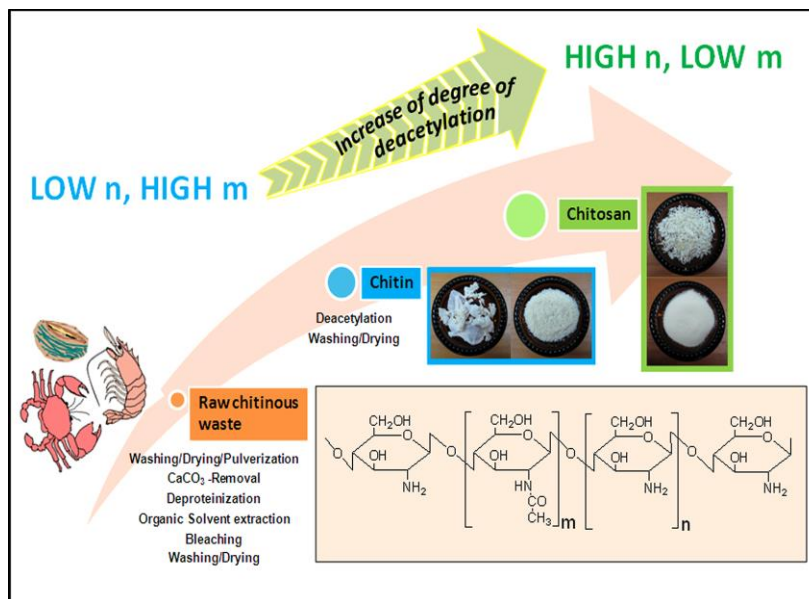


Figure 8 : Degrees of acetylation and deacetylation of chitin and chitosan. For chitin m , the number of acetamido groups, is larger than n , the number of free amino groups, while for chitosan $n > m$. Degrees of deacetylation and acetylation are $(n/(n + m)) \times 100$ and $(m/(n + m)) \times 100$, respectively.⁷

The pK_a of chitosan depends on the DD and it varies between 6.46 and 7.32. Chitosan with a smaller DA (higher DD) exhibits much better diverse biological properties than chitosan possessing a greater DA. Commercial chitin comes as whitish powder, flakes, beads, or nanoscale whiskers typically with 75–95% acetylation.¹⁰

The hydroxyl groups in chitin and chitosan contribute strong intra and intermolecular hydrogen bonds. In addition, both hydrophobic and hydrophilic interactions may occur between macromolecule chains. The linearity of chitin makes it easy for the molecules to produce strong intermolecular forces and results in a high degree of crystallinity.¹⁰ Molecular arrangement of α -chitin is favorable for the formation of strong inter-molecular hydrogen bonding, and thus it is the most stable form of the three crystalline variations.

1.7 Applications of Chitin and Chitosan

Interest in the commercial applications of chitin grew in the 1930s and early 1940s, but took a backseat for many years because synthetic polymers have been used for the applications. However, large-scale production of chitin was begun in the mid-70s when regulations were introduced to limit the dumping of untreated shellfish waste in coastal waters. Since then, producing chitin from shell wastes became an economical way to comply with the regulations. Nevertheless, chitin science continues to grow, and the estimated global market for chitin and its derivatives is forecast to reach 63 billion US dollars by 2015.¹⁸

Today, chitin, chitosan, and their derivatives have been identified as versatile biopolymers for a broad range of medical, agricultural, veterinary medicine, food, textile and paper industries' applications.¹⁰ Chitin is non-toxic and biodegradable, and therefore more environmentally friendly than most synthetic polymers. Table 3 summarizes some of the applications of chitin and chitosan.¹⁴

Table 2: Applications of chitin, chitosan and its derivatives¹⁴

Area	Applications
Agricultural	Coating of fertilizers, pesticides, herbicides, and insecticides for their controlled release to soil Coating of seeds and leaves to prevent microbial infections As an elicitor and a protector material for plants As a controller of pre-harvest and postharvest diseases of horticultural commodities
Biomedical and Pharmaceutical	Tissue engineering, drug and gene delivery fields, ranging from skin, bone, cartilage, and vascular graft Lowering of serum cholesterol Application in enzyme and cell immobilizations As a biomaterial, as a material for the production of contact lenses, bandages, surgical stiches, and electrochemical biosensors ⁷
Cosmetics	Component of toothpaste, hand and body creams, and shampoos
Environmental	In drinking water and wastewater treatment Chitosan as flocculating and chelating agents For the removal of heavy metals and dyes As an ecological polymer (eliminates synthetic polymers and reduces odor)
Food Industry	Clarification of juices, production of biodegradable packaging films, antimicrobial agents, beverage clarification additives, flavor extenders, color and texture stabilizers, a feed supplement, a food additive, a food preservative, and as an extender of shelf life of fruits and vegetables. ¹³
Pulp and Paper Industry	As a carbonless copy paper, as a processing additive for surface treatment applications, and for incorporation into photographic papers.
Textile Industry	Inclusion of chitosan into mixtures, blends, and coatings of other textiles such as silk, wool, viscose, cotton, and others are based on chitosan's properties to repel water.

1.8 Adsorption

Adsorption is a surface-based process essentially an equilibrium process classified as physisorption. In physisorption, adsorbate adheres to the surface of the adsorbent through weak intermolecular interactions such as Van der Waals (VDW) forces. On the other hand, chemisorption is also a type of adsorption in which a molecule adheres to a surface through the formation of a chemical bond. Adsorption is quite different from absorption, which is not a surface based process. Adsorption occurs at relatively low temperature and involves low heat of energy, whereas absorption is opposite to those. This physical adsorption is the most common type of adsorption, which is reversible, and absorption is irreversible.¹⁴

1.8.1 Dye adsorption mechanism^{19, 20}

During the adsorption of dye over a porous adsorbent, the following four consecutive steps take place.

Step 1 : Transport of dye ions from the bulk solution to the external surface of the adsorbent

Step 2 : Film diffusion - External mass transfer across the film surrounding the adsorbent particles

Step 3 : Particle diffusion/pore diffusion - Transport of the dye ions into the pores of the adsorbent

Step 4 : Chemical reaction - Adsorption of the dye ions onto the interior pore surface of the adsorbent via physisorption or chemisorption.

Furthermore, the rate of an adsorption process is controlled either by external diffusion, internal diffusion or by both types of diffusion. The external diffusion controls the migration of the solute species from the solution to the boundary layer of the liquid phase. Internal diffusion controls the transfer of the solute species from the external surface of the

adsorbent to the internal surface of the pores of the adsorbent material. If the external diffusion is greater than internal diffusion, the rate is governed by particle diffusion. If the external diffusion is less than the internal diffusion, rate is governed by film diffusion.

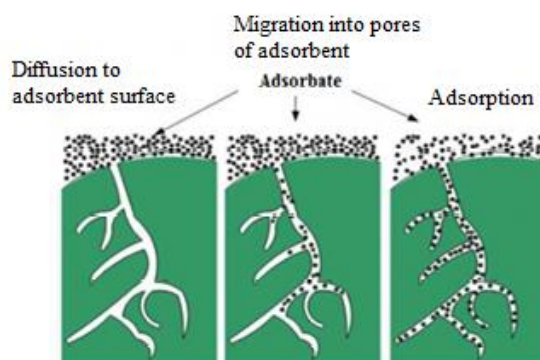


Figure 9: Three steps (1, 3 and 4) involved in adsorption mechanism²¹

After adsorption, a condition may cause the molecules to desorb. In some cases, adsorbed molecules may interact with active sites on the adsorbent pore surfaces and form the chemical bonds.

Because AY25 dye contains sulfonate groups and the chitin contains amino groups, the strong electrostatic interactions are expected for the main adsorption mechanism of acid dyes onto chitin. However, to have such an interaction, the ionization of sulfonate of AY25 dye and protonation of amide in chitin are required. Many studies have confirmed that the above process is favored under acidic conditions, where the total charge of chitin is more positive due to the stronger protonation of amino groups at acidic pH values.¹⁷ Thus, an increase in the DD facilitates the adsorption and generally gives an increase in adsorptive capacity for anionic dyes due to the availability of protonated amine groups.²²

1.8.2 Adsorption Kinetics

In the dye adsorption process, the kinetics and mechanisms are important for process control because they lead to information on the factors that affect the reaction rate, and the interactions that occur between the adsorbent and adsorbate.¹

Dye adsorption kinetics are influenced by sorption reactions and mass transfer steps (i.e. external and intra-particle diffusion). These steps depend on the physical form of the chitin (eg. particle size), the intrinsic structure of chitin (DA and DD, crystallinity, and molecular weight), the nature of the dye solution, as well as process conditions (temperature and pH). Simplified models can be used to test experimental data and identify the rate-controlling mechanism for adsorption process. Of these models, pseudo-first order, pseudo-second order, and intra-particle diffusion models are the most widely used models that have been used to describe the sorption of dye molecules onto chitin.^{14,23} This information is useful for further applications of system design in the treatment of natural water and waste effluents. The main kinetic equations are shown in Table 3. More detail about these models are discussed in section 4.5.

In this study we used pseudo-first order, pseudo-second order and intra particle diffusion models to analyze the kinetic behavior of AY25 dye onto chitin.

Table 3: Kinetic model equations used for dye adsorption process.²³ q_e and q_t are the adsorption capacities at equilibrium and at time t respectively.

Model	Equation	Description
Pseudo-first order equation of Lagergren	$\frac{dq_t}{dt} = k_1(q_e - q_t)$	k_1 is the pseudo-first order adsorption rate constant
Pseudo-second order equation	$\frac{dq_t}{dt} = k_2(q_e - q_t)^2$	k_2 is the pseudo-second order adsorption rate constant
Intra particle diffusion	$q_t = k_p t^{1/2} + C$	k_p is the intra particle diffusion rate constant

1.8.3 Adsorption isotherms

Adsorption is usually described by isotherms, which indicate how much solute can be adsorbed by the adsorbent at a given temperature. An adsorption isotherm relates the concentration of solute on the surface of the adsorbent to the concentration of the solute in the solution with which the adsorbent is in contact. These values are usually determined experimentally, but there are models to predict them, both for single adsorption and multicomponent adsorption.¹⁴

Although the Langmuir and Freundlich adsorption isotherms are the two well established types of adsorption isotherms for single component adsorption, there are other models including the consideration of adsorption equilibrium. For example, Table 4 lists the main adsorption equations used to elucidate the adsorption mechanism. They are described in detail in sections 4.6.2 to 4.6.5. In each case, q_e is the adsorption capacity at equilibrium and C_{eq} is the equilibrium concentration of the adsorbate in solution.

Table 4: Equations of adsorption isotherm models at equilibrium¹⁴

Isotherm	Equation	Description
Freundlich	$q_e = KC_{eq}^{1/n}$	K = Freundlich constant 1/n = Heterogeneity factor
Langmuir	$q_e = \frac{q_{e,max}bC_{eq}}{1+bC_{eq}}$	$q_{e,max}$ = maximum adsorption capacity b = Langmuir constant
Temkin	$q_e = \frac{RT}{b_T} \ln(A_T C_{eq})$	R = universal gas constant T = absolute temperature A_T and b_T are constants
Dubinin – Radushkevich (D-R isotherm)	$q_e = q_D \exp(-B_D \varepsilon^2)$	q_D = Dubinin–Radushkevich monolayer capacity B_D = constant related to the mean free energy of sorption per mole of the sorbate ε = Polanyi potential which is related to equilibrium concentration

1.8.4 Types of adsorption¹⁴

Isotherms of physical adsorption can be divided into five types. Figure 10 shows the shapes of curves for these five types of adsorption. Y-axis represents the amount of adsorbate adsorbed per unit amount of adsorbent (q_e) whereas X-axis represents the equilibrium concentration or relative pressure of adsorbate.

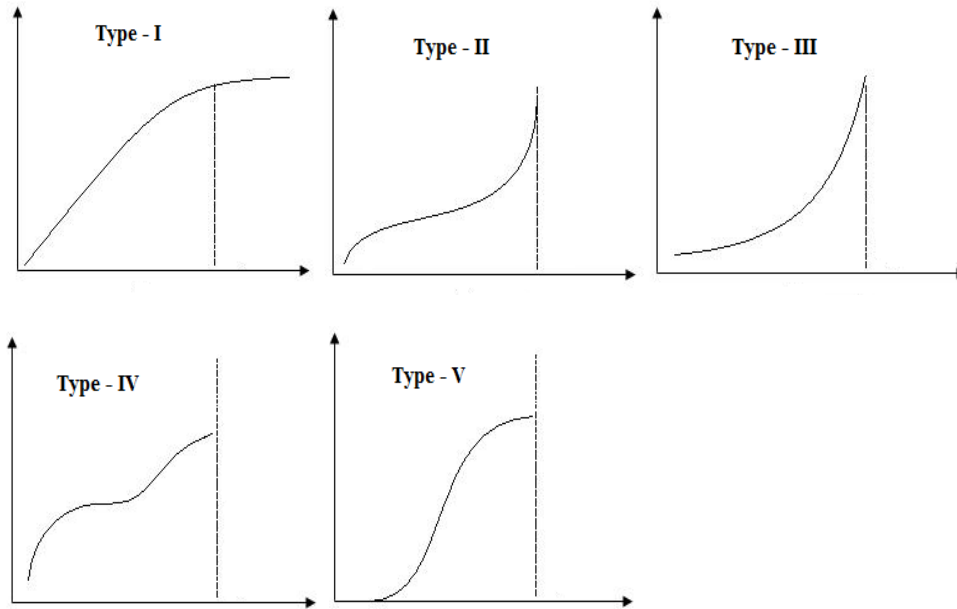


Figure 10: Types of characteristic isotherms²⁴

Type I is the typical Langmuir isotherm exhibited by unimolecular adsorption and applies to nonporous, microporous and adsorbents with small pore sizes (not significantly greater than the molecular diameter of the adsorbate).¹⁷ Type II and III adsorption isotherms show large deviation from Langmuir model. There is no flattish portion in the curves which indicates that monolayer formation is missing. In Type II, the lower pressure or concentration region of graph is quite similar to Type I, indicating the formation of monolayer followed by multilayer. Types II and III are observed in adsorbents with a wide range of pore sizes. Type III isotherm indicates the formation of multilayer. Type IV suggests the formation of two distinct surface layers with the intermediate flat region corresponds to monolayer formation. Type V is only when the intermolecular attraction effects are large.

1.9 Merit of the Research

Because of rapidly growing interest in the amino polysaccharide chitin as a functional biopolymer, a recent progress of basic and application studies in chitin chemistry is reviewed. Our main goal is to study the dye adsorption capability of chitin, particularly for the potential of AY25 dye removal

This study is mainly based on finding a simple, efficient and inexpensive way of removing dyes from waste waters. At first glance, chitin extracted from waste crab legs is chosen as an adsorbent material for removal of AY25 dye due to the high abundance of raw material for chitin extraction. The purified chitin was characterized using FTIR and XRD methods. Then the suitability and effectiveness of chitin for removal of AY25 dye is determined by performing series of batch experiment test. Our purpose is to determine the adsorptive capacity of chitin on AY25 dye. Second, the effect of initial dye concentration and adsorbent dosage are determined to optimize the process conditions for high efficiency. Unprocessed chitin and chitin extracted from red lobster shells are also tested to compare the most cost effective adsorbent.

To control the adsorption process, it is important to study the kinetics and mechanism of dye adsorption. Therefore equilibrium and kinetic experiments at different initial dye concentrations and chitin dosages are performed. Simplified kinetic models will be applied to determine the rate-controlling mechanisms for the adsorption process. Also the experimental data will be tested with the Langmuir, Freundlich, Temkin and D-R adsorption isotherm models. The nature of the adsorption is evaluated by using the calculated isotherm parameters.

CHAPTER 2

REVIEW OF LITERATURE

2.1 Previous research related to dye removal

Researchers have studied the adsorption method for removal of different dyes using various adsorbents. They have determined the capability of dye removal by calculating the adsorptive capacities of different adsorbents. Table 5 summarizes the adsorptive capacities of different adsorbents obtained from literature.

Table 5: Adsorptive capacities of different adsorbents on various dyes

Adsorbent	Dye	Adsorptive capacity (mg/g)	Process condition
Date stone ²⁵	Acid green 25 (AG25)	36	pH =2, 25°C
	Acid black 26 (AB26)	40	
	Acid blue 7 (AB7)	33	
Chitin ¹	Tartrazine (FD&C yellow 5)	30	pH =3, 25°C
Chitosan ¹	Tartrazine (FD&C yellow 5)	350	
Chitosan ¹	FD&C Red 40	90	pH=7.4
		360	pH=5.7
Chitosan (DD ^a = 82%)	Remazol Brilliant Blue RN (RB) ¹⁷	398	pH=2, 25°C
	Basic Blue 3G (BB) ¹⁷	254	pH=2, 25°C
Activated Carbon (SAE-2)	Remazol Brilliant Blue RN (RB) ¹⁷	475	pH=2, 25°C
	Basic Blue 3G (BB) ¹⁷	295	pH=2, 25°C
Chitosan ²⁶	Crystal violet	28.5	
Bentonite ²⁷	Basic red 2 (BR2)	274	30°C

Researchers have also focused their attention to study the equilibrium isotherms, kinetics, and mechanism of dye adsorption. Some of the examples of previously studied dyes are given below.

2.1.1 Tartrazine

Tartrazine is a food azo dye associated with most allergic and intolerance reactions. It is also considered toxic and can act as a catalyst in hyperactivity and other behavioral problems.¹ Therefore, the capability of removal of this dye from waste water using chitin obtained from shrimp has been investigated. Also the kinetics and mechanisms of tartrazine adsorption onto chitin at different pH values (3, 5, 7, 9 and 11) were studied. Results showed that the adsorption of tartrazine onto chitin was a very fast process, reaching the maximum adsorption capacity in about 10–15 min. Adsorption capacity was increased with pH decrease, reaching maximum values at pH 3. The maximum value was 30 mg/g for chitin. The pseudo-first order model showed a good fit with the experimental data. Mechanism study showed that the tartrazine adsorption onto chitin occurred only by film diffusion and via chemical interactions at pH 3. Table 6 summarizes the kinetic parameters for tartrazine adsorption onto chitin.¹

2.1.2 Verofix red

It was reported that adsorption of Verofix red dye onto chitin follows the pseudo first order kinetic and the rate parameters are shown in Table 6.²⁸

Table 6: Kinetic parameters for dye adsorption onto chitin^{1, 28}

Adsorbent	Dye	Pseudo first order			Pseudo second order			Experimental Condition
		k_1 (min^{-1})	q_{max} (mg/g)	R^2	$k_2 \times 10^3$	q_{max} (mg/g)	R^2	
Chitin	Tartrazine	0.297	30.5	0.994	17.6	31.8	0.951	pH=3, 25°C, Particle size = 68 to 75 μm , 100 rpm, Dye concentration = 100 mg/L
Chitin 1.0 g/L 1.5 g/L 2.0 g/L 2.5 g/L	Verofix red	0.144 0.166 0.167 0.175	27.54 30.2 33.89 37.15					pH = 6.7, 30°C, Particle size = 0.384 mm

2.1.3 Acid Yellow 25

Biotransformation of Acid Yellow 25 has been carried out using *Marinobacter gudaonensis* AY-13 isolated from natural marine environment. The % decolorization of Acid Yellow 25 was 92.00% and 90.03% in nutrient broth and half strength nutrient broth having 8.0% salt concentration respectively in 24 hours. The % decolorization of the dye by cell-free extract was found to be up to 80.13 % in 24 hours. The decolorization of the dye has also been studied in presence of different co-substrates (1% glucose, 1% yeast extract and 1% starch) and found that percent decolorization was up to 92.77%, 94.00% and 92.05% respectively. These results concluded that the isolate AY-13 could decolorize the dye very effectively. Degradation products of Acid Yellow 25 were non-toxic to ecologically important microorganisms.²

2.1.4 Reactive dye Black 5 (RB5)

Several research groups have reported kinetic and isotherm parameters related to RB5 in different experimental conditions. One finding is that the adsorptive capacity of RB5 onto

chitin was 19 mg/g to 162 mg/g. The best results were achieved at pH 3, 200 rpm and 2 h contact time.²⁹ Results showed that experimental data were best fitted with the Langmuir isotherm model and the isotherm parameters are shown in Table 7.

Table 7: Langmuir isotherm parameters for RB5 adsorption onto chitin²⁹

pH	Amount of chitin					
	1 g/dm ³			5 g/dm ³		
	b dm ³ /mg	q _{max} mg/g	R ²	b dm ³ /mg	q _{max} mg/g	R ²
3	0.5	160	0.986	0.25	100	0.993
5	0.09	21	0.994	0.017	21	0.995
9	0.07	19	0.993	0.01	18	0.994

Begum et.al (2012) reported that RB5 dye adsorption onto chitin extracted from shrimp followed the Langmuir isotherm and it was a pseudo second order reaction at pH 3.2 and at 30 °C.³⁰ Kinetic and isotherm parameters related to this study are summarized in Tables 8 and 9.

Table 8: Kinetic parameters for RB5 dye adsorption onto chitin

Kinetic parameters	RB5 Initial dye concentration (mg/L)		
	30	40	50
q _{e,exp} (mg/g)	24.98	32.86	41.82
Pseudo-first order			
k ₁ (min ⁻¹)	19.8	18.42	11.95
R ²	0.9759	0.9905	0.9719
q _{e,max}	18.62	23.99	34.67
Pseudo-second order			
k ₂ × 10 ⁴ (g.mg ⁻¹ .min ⁻¹)	9.12	6.76	4.07
R ²	0.9978	0.9974	0.9904
q _{e,max}	27.03	35.71	43.45

Table 9: Langmuir and Freundlich isotherm parameters for RB5 dye adsorption onto chitin at different temperatures

Temperature (K)	Freundlich	Langmuir		
	R ²	R ²	q _{max} (mg/g)	b
303	0.7775	0.9998	38.49	2.2
311	0.9680	0.9997	41.3	1.5
319	0.7559	0.9999	46.44	1.81
327	0.6869	0.9990	57.36	2.72

2.1.5 Reactive Yellow 2 (RY2) and Reactive Black 5 (RB5)

Experiments have been carried out using 0.2 g of chitin in 50 mL of dye solution at 293 K and 333 K (pH = 6.94, 300 ppm for RY2 and pH=7.12, 600 ppm for RB5). Results showed that RY2 dye adsorption onto chitin is a physisorption process and RB5 adsorption is a chemisorption process.³¹ Kinetic parameters for both dyes are given in Table 10.

Table 10: Kinetic parameters related to the adsorption of RY2 and RB5 onto chitin

Kinetic parameters	RY2		RB5	
	293 K	333 K	293 K	333 K
Pseudo-first order k ₁ ×10 ³ (min ⁻¹) R ²	2.7 0.9503	36.9 0.9995	3.91 0.9588	4.29 0.9820
Pseudo-second order k ₂ ×10 ⁴ (g.mg ⁻¹ .min ⁻¹) R ²	4.66 0.9948	23.4 0.9998	3.98 0.9839	3.26 0.9415
Intra particle diffusion k _p (mg .g ⁻¹ min ^{-1/2}) R ²	1.00 0.9988	2.83 0.9963	1.65 0.9984	1.88 0.9988

Even though there are many records of different dyes available in literature, there is no research conducted to remove AY25 dye using chitin. Therefore, our research group was

interested in investigating the method of removal of this dye studying the isotherms and kinetics of AY25 dye adsorption onto chitin.

CHAPTER 3

EXPERIMENTAL

3.1 Extraction of Chitin

3.1.1 Preparation of raw materials

Waste snow crab (*Chionoecetes opilio*) legs were obtained from Dierbergs Sea Food market (Edwardsville, IL). The loose tissues inside the crab legs were scraped and shells were washed thoroughly with water and finally with deionized water. Shells were dried at room temperature (23 °C) for 2 to 3 days. Dried shells were ground using a regular coffee grinder (MR.COFFEE, Model-IDS77) until it became fine powder. Figure 11 shows the raw crab legs (A), dried crab shells (B) and crab shell powder (C), respectively.

3.1.2 Demineralization

Demineralization was performed using 0.25 M HCl solution at room temperature (~23 °C) with a solution to solid ratio of 40 mL/g.¹¹ 400 mL of 0.25 M HCl was added to the 10 g of dried crab shell powder and the mixture was stirred (Barnstead/Thermolyne, Cimarec, Model-SP131325) for 30 minutes at 23 °C (Figure 11D). After a 30 minute period, the supernatant was decanted off and the treatment was repeated three times. The solution was filtered (Whatmann filter paper 8) using suction filtration after the third treatment. The resulting solid was washed with deionized water until it became neutral (Figure 11E).

3.1.3 Deproteinization

Deproteinization was performed using 1.0 M NaOH at 70 °C with a solution to solid ratio of 20 mL/g.¹¹ 200 mL of 1.0 M NaOH was added to the demineralized product and the mixture was stirred for 30-45 minutes at 70 °C (Figure 11F). After that, the supernatant was decanted off and the treatment was repeated three times. The absence of proteins was indicated by the absence of color of the supernatant at the last treatment which was left overnight. The solution after the overnight treatment was filtered using suction filtration. The resulting solid was washed with deionized water until it becomes neutral.

3.1.4 Purification and sieving

Deproteinized product was washed with 100 mL of hot ethanol (~ 60 °C) and later boiled in 100 mL of acetone for 10-15 minutes.¹¹ The solution was filtered using suction filtration and the product was air dried. Dried chitin (Figure 11G) was passed through No. 50 and No. 80 (297-177 µm) U.S. Standard sieves. All experiments were performed using purified chitin retained on mesh No. 80 having a 297-177 µm range of particle size for homogeneity.

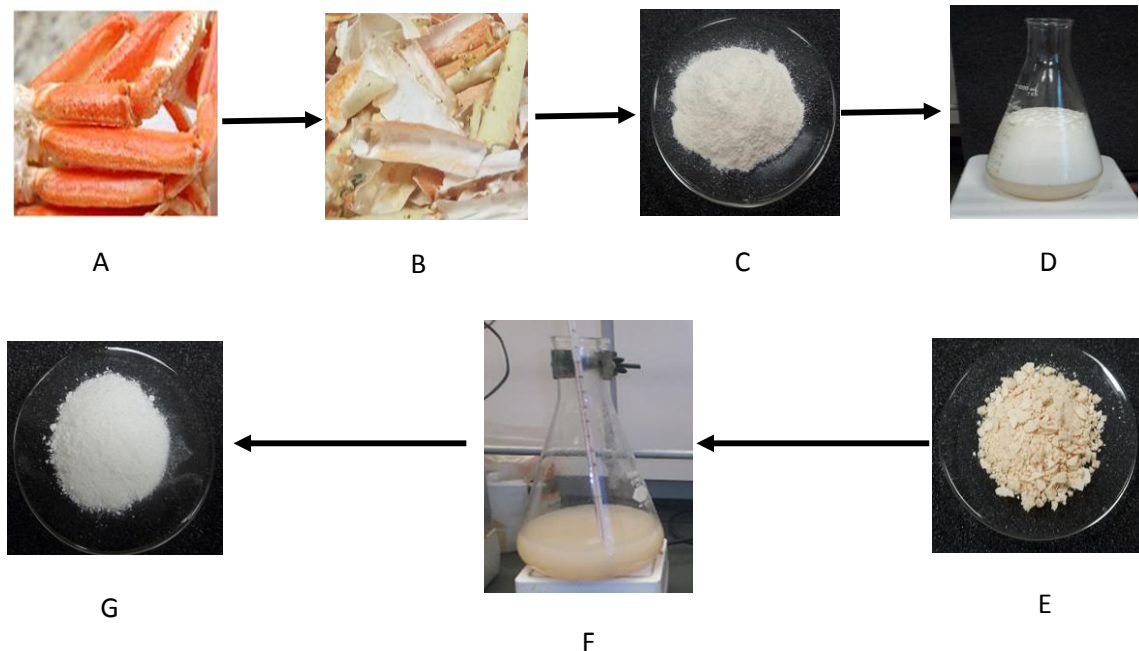


Figure 11: Scheme of the extraction of chitin from crab legs. (A) Raw crab legs, (B) Dried crab shells, (C) Crab shell powder after grinding, (D) Demineralization: crab shell powder reacts with 0.25 M HCl producing large volume of air bubbles, (E) Demineralized product after washing and drying, (F) Deproteinization: Stirring demineralized product with 1M NaOH at 70°C, (G) Purified chitin

3.2 Preparation of chitosan

Chitin extracted from crab legs was sieved into the 297-177 μm range of particle size. 50 % NaOH was added to chitin (10 mL/g) in a round-bottom flask. Deacetylation was facilitated by steeping in strong NaOH at room temperature (23 °C) for one day before heating.¹¹ Solution was then refluxed at 140 °C for 4 hours in a sand bath. The product was filtered using suction filtration and washed with distilled water until it becomes neutral. The product was oven dried at 40 °C (Labnet mini incubator) for 24 hours. The degree of deacetylation was calculated using Equation 1.

$$\text{Degree of deacetylation} = 100 - \frac{[A_{1655}] [100]}{[A_{3450}] [1.33]} \quad \text{Equation 1}^{14}$$

Where $[A_{1655}]$ and $[A_{3450}]$ are the absorbance at wavenumbers 1655 cm^{-1} and 3450 cm^{-1} respectively.

3.3 Characterization of Chitin/Chitosan

3.3.1 Fourier transform infrared spectroscopy (FTIR)

The Fourier transform infrared (FTIR) spectra of chitin and chitosan were measured over the frequency range 4000 to 400 cm^{-1} at resolution of 4 cm^{-1} using a Nicolet iS5 FT-IR spectrometer.



Figure 12: ATR-FTIR Spectrophotometer

3.3.2 X-ray powder Diffractometry (XRD)

The XRD measurement on powder chitin sample was carried out using a Rigaku MiniFlex+ X-ray diffractometer equipped with Ni-filtered $\text{Cu K}\beta$ radiation ($\lambda=1.5406\text{ \AA}$). The relative intensities were recorded between $2\theta = 5^\circ$ - 40° at room temperature ($23\text{ }^\circ\text{C}$). The X-ray diffractometer was operated with 1° diverging and receiving slits at 50 kV and 40 mA and a continuous scan was carried out with a step size of 0.015° and a step time of 0.2 second. Peaks were compared with the α -chitin peaks obtained from the MDI JADE data base.

3.4 Adsorption experiments

3.4.1 Batch treatment Test

Acid Yellow 25 (AY25) dye was purchased from Sigma Aldrich (St. Louis, MO). AY25 stock dye solution was prepared by dissolving 3 g of dye in 1000 mL of deionized water. Different concentrations of dye solutions (58, 165, 284, 385 mg/L) were prepared by diluting the stock dye solution with appropriate amount of deionized water. The pH of the solutions was adjusted to 2 by adding small amount of 3 M HCl or 3 M NaOH. The pH was measured using Accumet Basic AB15 pH meter. Batch experiments were performed using various amounts of chitin (0.1 g to 0.5 g) in Erlenmeyer flasks containing 100 mL of dye solution (pH= 2) at room temperature (23 °C). The flasks were placed on a shaker (New Brunswick Scientific, Edison NJ) at 70 rpm. 1 mL of dye solution from each flasks was withdrawn into eppendorf tubes at 15 minutes intervals for 150 minutes while shaking the flasks. Samples were centrifuged (Brinkmann centrifuge 5412) for 2 minutes. The absorbance of supernatant was monitored at 392 nm using a UV-1800 double-beam spectrometer (Shimadzu, Kyoto, Japan). A calibration curve was generated before each set of experiments using a series of dilution ranging from 0.0005 to 1 mM dye solutions. Concentration of each solution at 15 minutes interval was calculated using the calibration curve. The % dye removal was calculated using equation 2. The same set of experiments were carried out with various initial dye concentrations (58, 165, 284, 385 mg/L) in triplicate.

$$\% \text{ Removal of dye} = \frac{(C_i - C_f)}{C_i} \times 100 \quad \text{Equation 2}^{12}$$

Where C_i and C_f are the initial and final concentrations of dye.

The adsorption capacity at time t (q_t) was determined by Equation 3.

$$q_t = \frac{(C_o - C_t)V}{m} \quad \text{Equation 3}^1$$

Where C_o is the initial dye concentration in liquid phase (mg/L), C_t is the dye concentration in liquid phase at time t (mg/L), m is the amount of chitin (g), and V is the volume of solution (L). Effect of adsorbent dosage and initial dye concentration on AY 25 dye removal were studied using these data. Also kinetic studies were performed using the same data.

3.4.2 Adsorption isotherm test

Different concentrations of dye solutions (235, 323, and 385 mg/L) were freshly prepared by dissolving AY25 dye in appropriate amount of deionized water in volumetric flasks. pH of the solutions was adjusted to 2 by adding small amount of 12 M HCl. Various amounts of chitin (0.1, 0.2, 0.3, 0.4 and 0.5 g) were added to the Erlenmeyer flasks containing 100 mL of dye solutions (pH= 2). The flasks were shaken in a shaker (New Brunswick Scientific, Edison NJ) at 70 rpm at room temperature (23 °C). 1 mL of dye solution from each flasks was withdrawn into Eppendorf tubes after 150 minutes. Samples were centrifuged (Brinkmann centrifuge 5412) for 2 minutes. The absorbance of supernatant was monitored at 392 nm using a UV-1800 double-beam spectrometer (Shimadzu, Kyoto, Japan). Calibration curve was generated before each experiment using a series of dilution ranging from 0.0005 to 1 mM dye concentrations. Equilibrium dye concentration of each solution at 150 minutes was calculated using the calibration curve. Same set of experiments were carried out with various initial dye concentrations in triplicate in same experimental conditions.

Data from these adsorption experiments was used to interpret the Langmuir, Freundlich, Tempkin and D-R isotherm plots.

3.4.3 Adsorption experiments using unprocessed chitin

365 mg/L of dye solution was freshly prepared in volumetric flask. The pH of the solution was adjusted to 2 by adding small amount of 12 M HCl. Various amounts of chitin (0.1, 0.2, 0.3, 0.4 and 0.5 g) were added to the Erlenmeyer flasks containing 100 mL of dye solutions at pH= 2. The flasks were shaken at 70 rpm at room temperature (23 °C). 1 mL of dye solution from each flasks was withdrawn into eppendorf tubes after 150 minutes. Samples were centrifuged (Brinkmann centrifuge 5412) for 2 minutes. The absorbance of supernatant was monitored at 392 nm using a UV-1800 double-beam spectrometer (Shimadzu, Kyoto, Japan). Same set of experiments were carried out using unprocessed chitin (range of particle size = 297-177 μm) instead of chitin with the same dye solution at same experimental conditions. These experiments were repeated using 140 mg/L of dye solutions. Each experiments were performed in triplicate.

3.4.4 Effect of the source of chitin

To determine the effect of original source of chitin for dye adsorption, adsorption experiments were carried out using chitin extracted from crab legs as well as from red lobster shells. The same procedure given in 3.4.2 was followed with 58 mg/L of dye solution.

3.4.5 Statistical Analysis

Each experiment was performed in triplicate. Results are expressed as mean + standard deviation (SD). Linear regression fitting analyses were performed with Origin 7 software (OriginLab Corporation, Northampton, MA, USA).

CHAPTER 4

RESULTS AND DISCUSSION

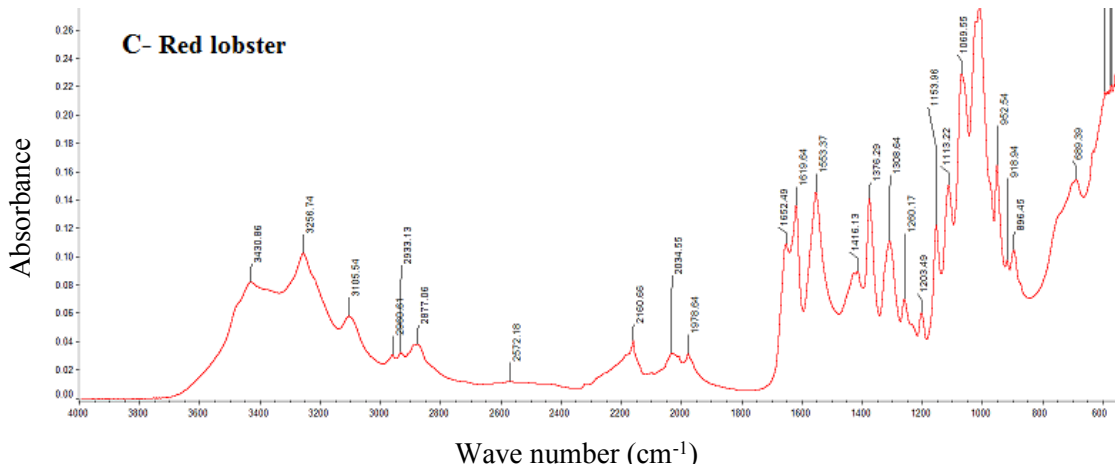
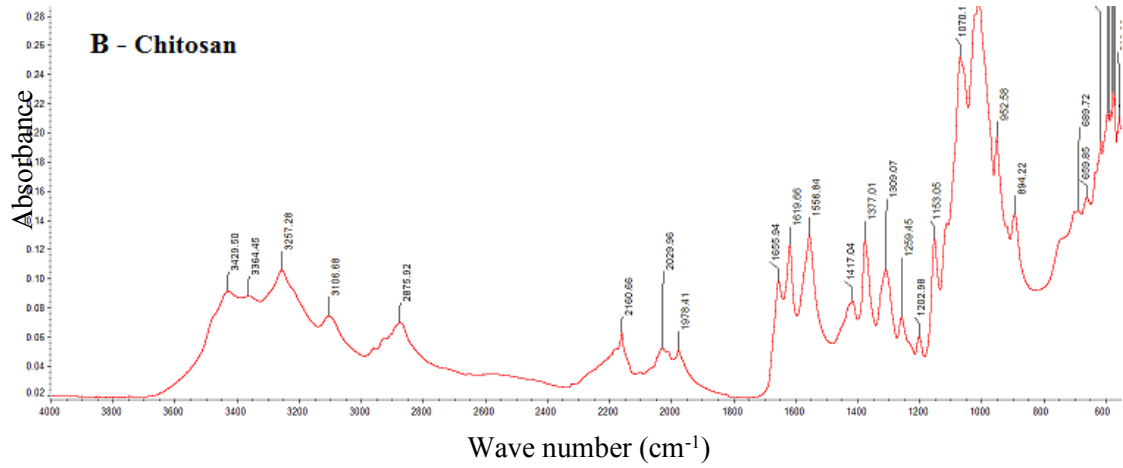
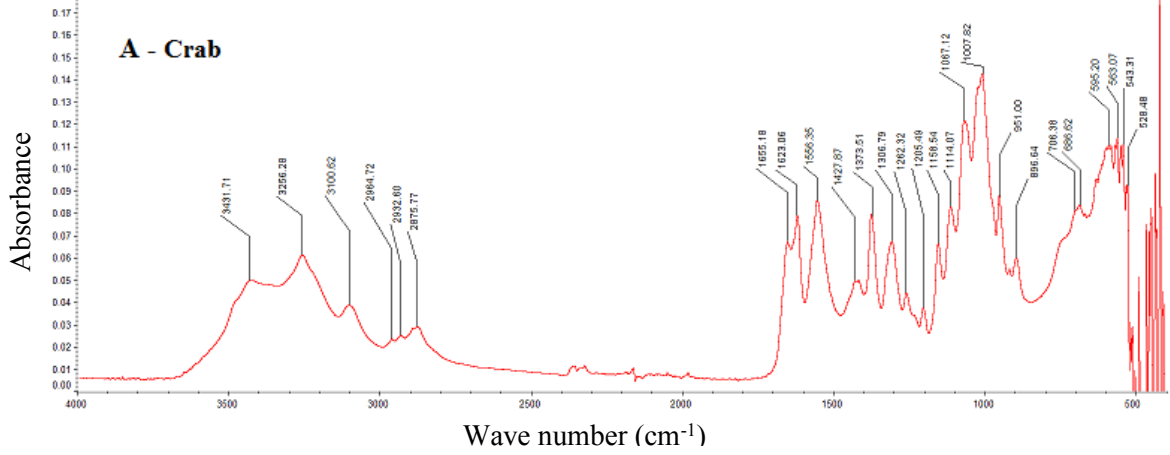
4.1 Extraction of chitin

Chitin was obtained from crab shells with a yield of ~28 %. Crab shells mainly consist of chitin, protein, and calcium carbonate with an average composition of 30, 30, and 40 % by weight respectively. This implies that the production of chitin was very high (approximately 93%) on the laboratory scale. The processes of washing, separation by sedimentation of solid and suction filtration are considered to be the main contributors to loss of bio-material.

The effectiveness of alkali deproteinization depends on the process temperature, the alkali concentration, and the ratio of its solution to solid material. The mineral, protein and color content in the exoskeleton are not the same for each species. The number of baths and their duration were dependent on the species. Therefore treatment time was increased when chitin was extracted from red lobster and a higher volume of ethanol and acetone were used to purify the chitin.

4.2 Characterization of Chitin

4.2.1 Fourier Transform Infrared Spectroscopy



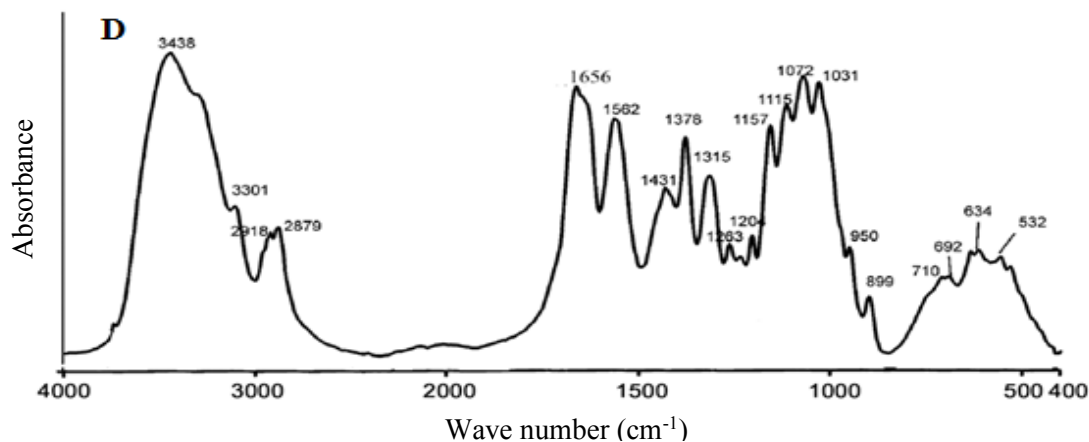


Figure 13: FT-IR spectra of chitin (A) and chitosan (B) extracted from crab legs, chitin extracted from red lobster shells (C), β -chitin from cuttlefish¹¹

Due to the different structural arrangement in α -chitin and β -chitin, different patterns occur in the IR spectra of α -chitin and β -chitin.¹¹ The band near 1650 cm^{-1} is due to the carbonyl stretching in amide group. Figure 13A and C confirms that the isolated chitin has α -chitin structure due to the splitting of amide band at 1655 cm^{-1} which is attributed to the presence of intermolecular hydrogen bond ($\text{CO}\dots\text{HN}$) and at 1625 cm^{-1} due to the intramolecular hydrogen bond ($\text{CO}\dots\text{HOCH}_2$). On the other hand, a single band is observed in β -chitin at 1656 cm^{-1} which is commonly assigned to the stretching of the CO group hydrogen bonded to amide group of the neighboring intra-sheet chain (Figure 13D).¹¹ The band due to NH stretching can be seen clearly at 3256 cm^{-1} and 3105 cm^{-1} in Figure 13A and C, confirming the α -chitin structure. Bands at 3256 cm^{-1} is due to the NH stretching which is intermolecularly bonded to carbonyl ($\text{CO}\dots\text{NH}$) and band at 3105 cm^{-1} is due to the H-bonded NH group. These bands are weak and not easily observed in β -chitin spectrum.¹¹ The bands around 1420 and 1065 cm^{-1} are attributed to $-\text{CH}_2$ bending and C-O stretching vibrations respectively. These remarkable differences between the two types of chitin is due to a relatively low crystallinity and loosely ordered structure showing weaker inter- and

intramolecular hydrogen bonding in β -chitin compared to that of the α -chitin. There is no significant difference observed in the IR spectra of chitin extracted from crab legs and red lobster shells.

In the IR spectrum of chitosan (Figure 13B), higher absorbance corresponding to the hydroxyl band was observed with compared to that of chitin. Degree of deacetylation (DD) was calculated using the absorbance values at 1655 and 3450 cm^{-1} and equation 1. The maximum DD value we observed was $\sim 20\%$.

4.2.2 X-ray Powder Diffractometry (XRD)

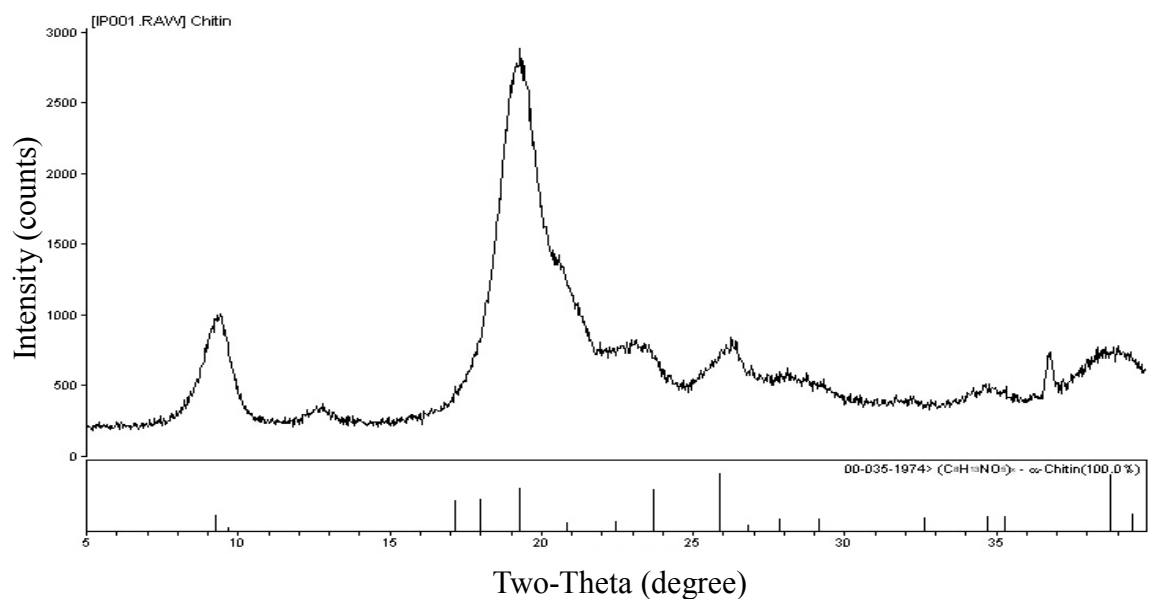


Figure 14: XRD patterns of chitin extracted from crab legs- Vertical lines shown below the XRD spectrum are relevant to the major peaks observed in α -chitin structure obtained from MDI JADE data base.

XRD analysis is used to detect the crystallinity of the isolated chitin. Depending on the source of raw material, different XRD patterns have been observed.¹¹ The XRD patterns of chitin extracted from crab legs confirms that chitin is in its α -form as five sharp crystalline reflections at 9.3°, 19.3°, 23°, 26° and 36.7° are comparable to the XRD patterns for α -chitin in MDI JADE data base and the literature. The reflection around 9-11° is associated with the

most ordered region involving the acetamide groups, and its intensity reflects the hydrated crystal content.

There is a significant difference between the XRD patterns of α -chitin and β -chitin. This is because of the different arrangements adopted by these polymorphs. The XRD profile of the α -chitin exhibits well-resolved and intense peaks at 9.6° and 19.6° , while a broad diffuse scattering and less intense peaks are found for the β -chitin.¹¹ This indicates that α -chitin is a more crystalline polymorph because of its antiparallel compact structure.

4.3 Effect of adsorbent dosage on AY25 dye removal

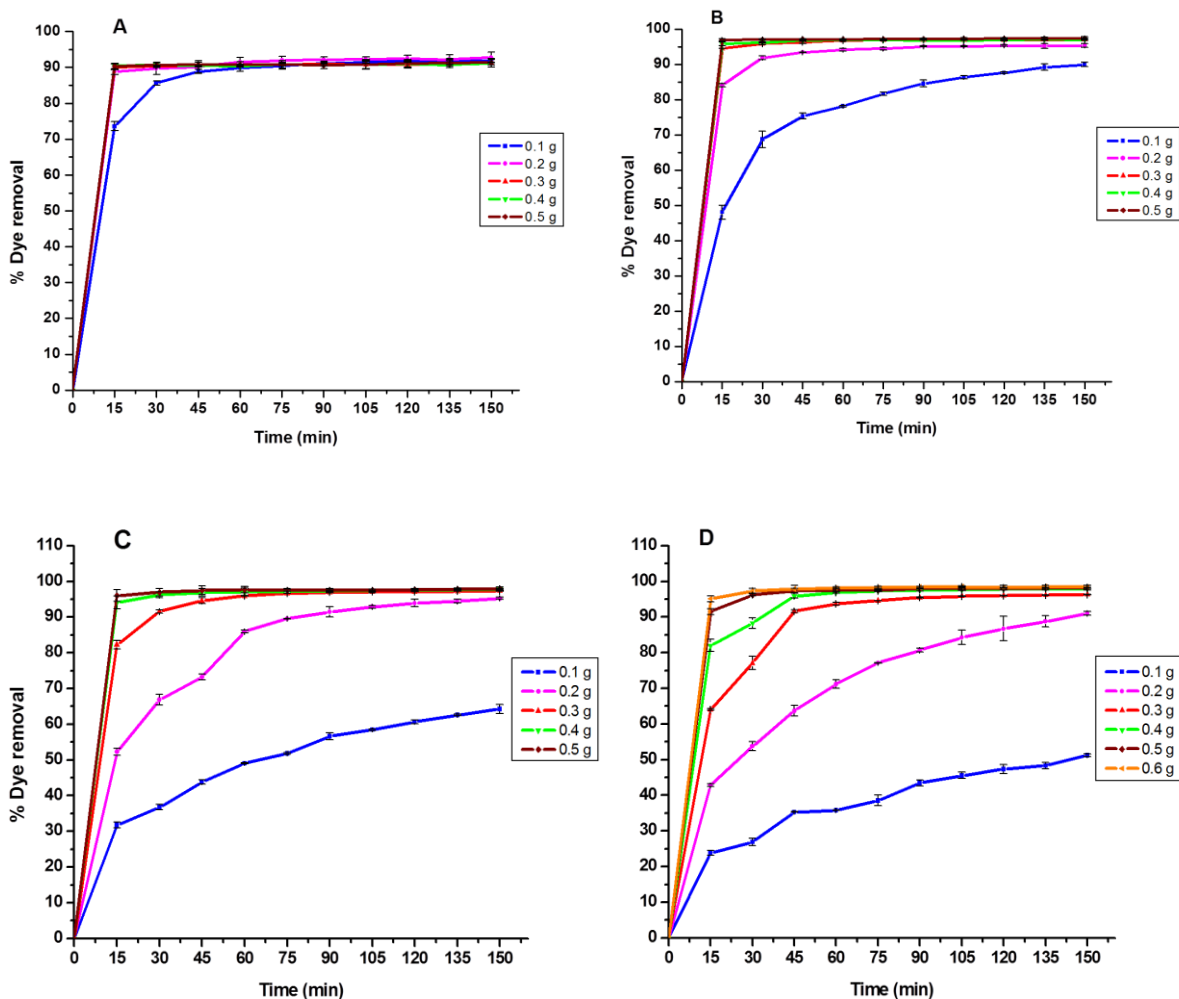


Figure 15: Effect of adsorbent dosage on AY25 dye removal
 Temperature = 23°C, pH = 2, Volume of dye solution = 100 mL, Shaking rate = 70 rpm, Range of particle size = 297-177 μm , Initial dye concentration = 58 mg/L (A), 165 mg/L (B), 284 mg/L (C), 385 mg/L (D), Amount of chitin vary (0.1, 0.2, 0.3, 0.4, and 0.5 g)

It is expected that the increase in adsorption with adsorbent dosage is attributed to an increased adsorbent surface and the availability of more adsorption sites. However, if the adsorption capacity is in milligrams of dye adsorbed per gram of adsorbent (Equation 4), the capacity decreases with the increasing amount of adsorbent.

At low initial dye concentration (Figure 15A), the adsorption of dye onto chitin is very effective and reaches equilibrium very quickly. Since the ratio of dye to chitin is lower, the observation indicates the possible formation of monolayer coverage of the dye molecules at the outer surface of the chitin. At an initial dye concentration of 58 mg/L, all chitin dosages were sufficient to remove 90% of dye within 15 minutes contact time except for chitin dosage of 0.1 g. When the initial dye concentration was increased to 165 mg/L, at least 0.3 gram of chitin is required to remove 90% of dye within 15 minutes. The same trend was observed at higher initial dye concentrations of 284 mg/L and 385 mg/L. With the increase in dye concentration, low chitin dosages (0.1 and 0.2 g) are not sufficient to achieve 90% dye removal within 60 minutes.

4.4 Effect of initial dye concentration on adsorptive capacity

4.4.1 Adsorptive Capacity

Adsorptive capacity at equilibrium (q_e) is a measurement of how well a certain adsorbent adsorbs the adsorbate in solution. This term is for a better comparison and important to judge the performance of an adsorbent. The value of q_e can be calculated using the equation shown below.

$$\text{Adsorptive Capacity } (q_e) = \frac{\text{Amount of dye adsorbed (mg)}}{\text{Amount of Chitin (g)}} \quad \text{Equation 4}^{32}$$

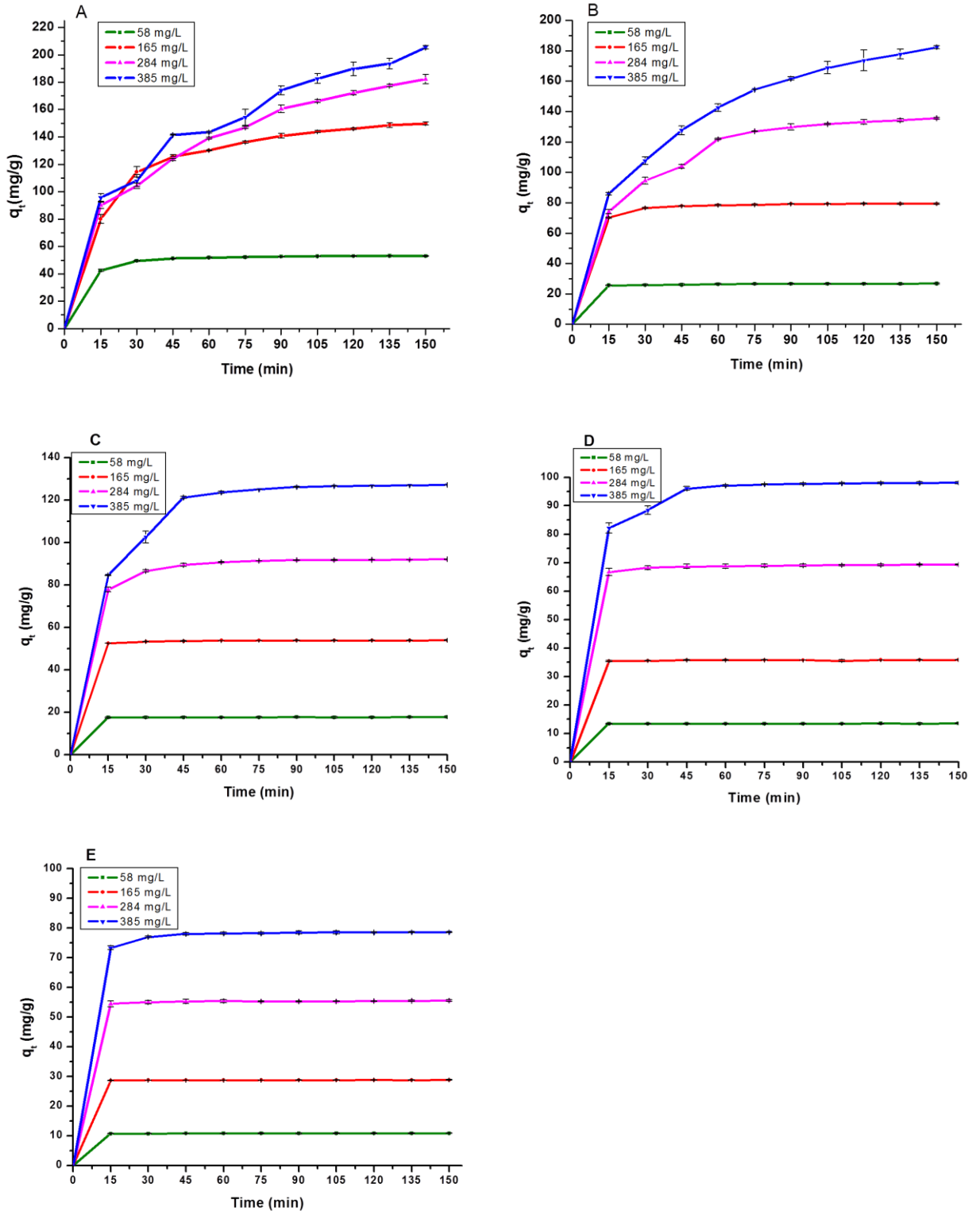


Figure 16: Effect of initial dye concentration on adsorptive capacity
23°C, pH = 2, Volume of dye solution = 100 mL, Shaking rate = 70 rpm, Range of
particle size = 297-177 μ m, Amount of chitin 0.1 g (A), 0.2 g (B), 0.3 g (C), 0.4 g (D),
0.5 g (E). Green, red, pink and blue colors show the initial dye concentrations
of 58, 165, 284 and 385 mg/L respectively.

According to the results shown in Figure 16, the initial dye concentration plays an important role in adsorptive capacity. The amount of dye adsorbed onto chitin increases with an increase in the initial dye concentration at a constant amount of adsorbent. Same trend was observed with different chitin amounts. However, with the increase of chitin dosage (Figure 16A to E), adsorptive capacity was decreased for all the initial dye concentrations. This is expected because there are plenty of chitin surface available for the limited amount of dye molecules. In other words, at lower dye concentrations, the ratio of initial number of dye molecules to the available adsorption sites is low. At higher dye concentrations, this ratio becomes higher, and subsequently the removal of dye depends on the initial concentration. Overall, the adsorption of AY25 dye onto chitin is a very fast process, reaching the maximum adsorption capacity (q_e) within 45 minutes with the chitin dosage of at least 0.3 g for all initial dye concentrations.

As shown in Figure 16, the amount of dye adsorbed onto chitin increases with time. However, at certain time points, it reaches a constant value, beyond which no more dye is further removed from the solution. At this point, the amount of dye desorbing from chitin is in a state of dynamic equilibrium with the amount of dye being adsorbed and desorbed onto and from chitin. In other words, fast diffusion into the external surface of the adsorbent was occurred by a fast pore diffusion into the intra particle matrix to attain rapid equilibrium.

4.5 Adsorption Kinetics

We used simplified kinetic models to determine the adsorption kinetics and mechanisms (potential rate-controlling steps, such as external and intra particle mass transfer). These models include the pseudo-first order, pseudo-second order, and intra

particle diffusion equations.¹⁴ The best fit was estimated in terms of the coefficient of determination, R^2 .

4.5.1 The Pseudo-first order equation

Pseudo-first order model assumes that the adsorption occurs due to a concentration difference of the adsorbate between adsorbent surface and solution. Therefore, this process occurs only by the external mass transfer coefficient.¹

The Lagergren rate equation is the first rate equation for adsorption in a liquid/solid system based on solid capacity. It is given in Equation 5.

$$\frac{dq_t}{dt} = k_1(q_e - q_t) \quad \text{Equation 5}^{14}$$

After integration on both sides of the equation and applying conditions for $q_t = 0$ at $t = 0$ and $q_t = q_t$ at $t = t$, the Equation 6 can be used for the kinetic analysis of experimental results.¹⁴

$$\log(q_e - q_t) = \log q_e - \frac{k_1}{2.303} t \quad \text{Equation 6}^{14}$$

Where

- q_e = Amount of dye adsorbed at equilibrium (mg/g)
- q_t = Amount of dye adsorbed at time t (mg/g)
- k_1 = Equilibrium rate constant of pseudo-first order kinetics (min^{-1})

From the equation, we expect to see a linear curve when $\log(q_e - q_t)$ versus t was plotted. The slopes of the plots then corresponds to the value of k_1 . The data are shown in Figure 17 and apparently the adsorption of AY25 onto chitin does not follow pseudo-first order model. Nevertheless, The applicability of pseudo-first order model for the adsorption of AY25 dye onto chitin at different initial dye concentrations (58, 165, 284, and 385 mg/L)

were tested by plotting $\log (q_e - q_t)$ versus t . The k_1 , the calculated q_e ($q_{e,cal}$) and the coefficient of determination (R^2) were calculated and are given in Table 11.

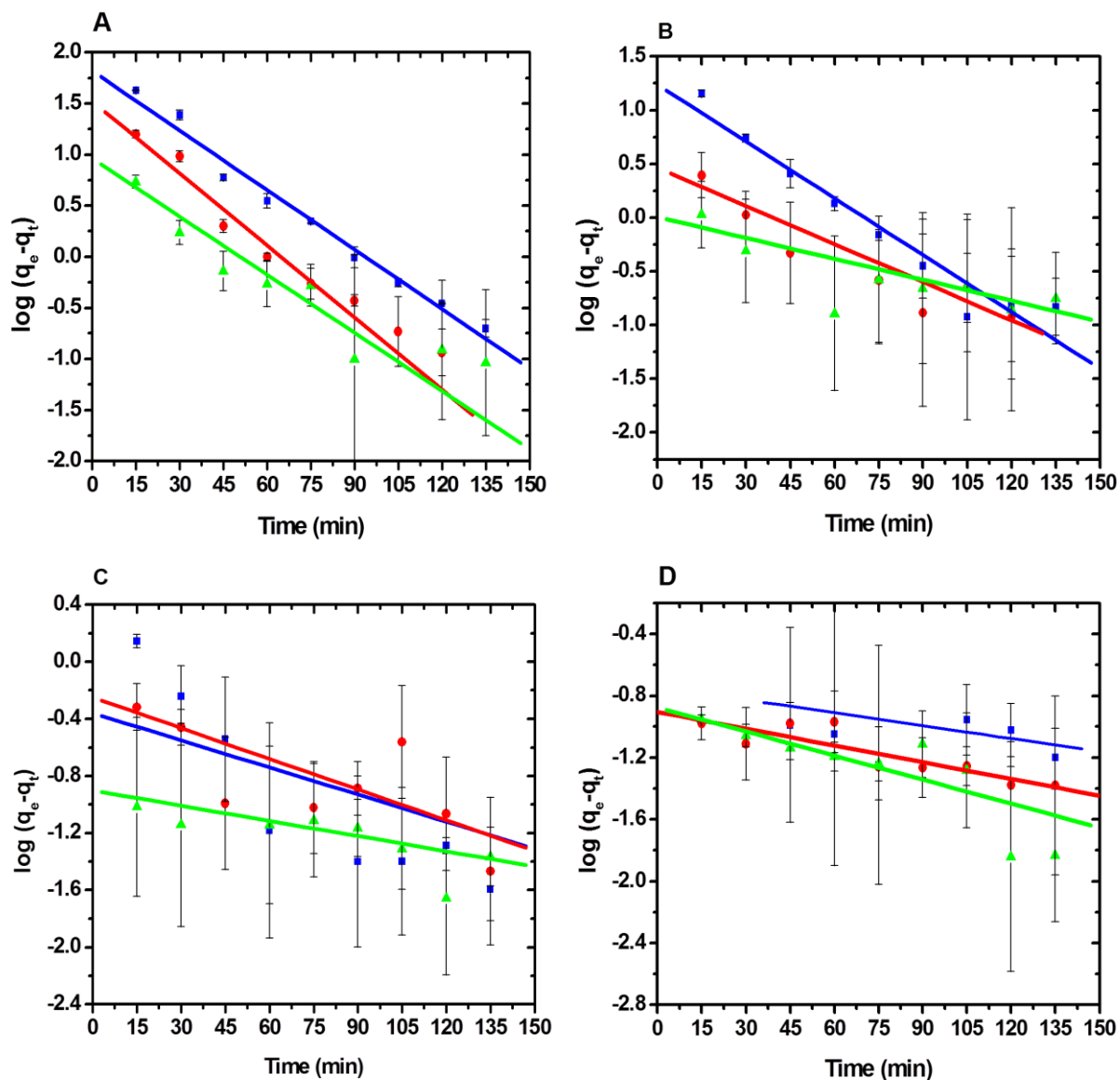


Figure 17: Pseudo-first order kinetic model for AY25 dye adsorption onto chitin. At 23 °C and in different initial dye concentrations (A) 385 mg/L, (B) 284 mg/L, (C) 165 mg/L, (D) 58 mg/L. Blue, red and green marks represent the chitin dosages of 3, 4, and 5 g/L

4.5.2 The Pseudo-second order equation

Then we attempted to fit our data with pseudo-second order equation. The pseudo-second order kinetic rate equation is given below.

$$\frac{dq_t}{dt} = k_2(q_e - q_t)^2 \quad \text{Equation 7}^{14}$$

Where k_2 is the equilibrium rate constant of the pseudo-second order kinetic model ($\text{g mg}^{-1} \text{ min}^{-1}$). After integrating Equation 7, the following equation can be obtained.

$$\frac{t}{q_t} = \frac{1}{k_2 q_e^2} + \left(\frac{1}{q_e}\right) t \quad \text{Equation 8}^{20}$$

To determine the applicability of the model, linear plots of t/q_t versus t for the adsorption of AY25 dye onto chitin at different dye concentrations (385, 284, 165, and 58 mg/L) were plotted to obtain the rate parameters. The k_2 , the calculated q_e ($q_{e,cal}$) and the coefficient of determination (R^2) were calculated and are given in Table 11.

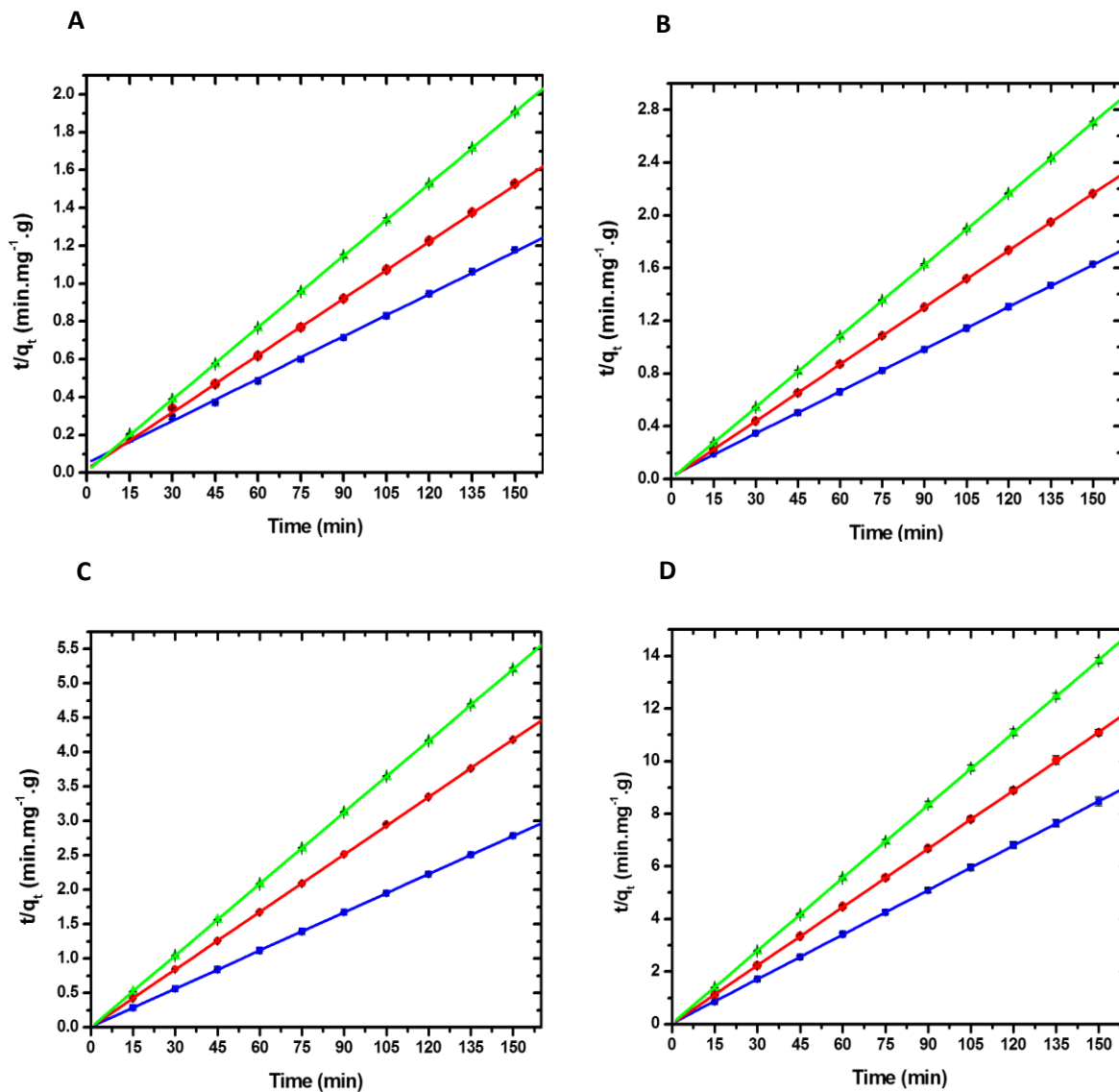


Figure 18: Pseudo-second order kinetic model for AY25 dye adsorption onto chitin. At 23 °C and in different initial dye concentrations (A) 385 mg/L, (B) 284 mg/L, (C) 165 mg/L, (D) 58 mg/L. Blue, red and green lines represent the linear fit for chitin dosages of 3, 4 and 5 g/L

Our experimental data do not show a good linear fit using pseudo-first order kinetic model. Also the obtained experimental q_e ($q_{e,exp}$) values, determined from the time at 135 min, do not agree with the calculated ones ($q_{e,cal}$). On the other hand, a linear fit for t/q_t versus contact time (t) was observed using pseudo-second order kinetics as shown in Figure

18 and the fitted results are shown in Table 11. Our results revealed that the dye removal kinetics can be approximated as a pseudo-second order kinetic model. In addition, the experimental q_e ($q_{e,exp}$) values agree with the calculated ones ($q_{e,cal}$) obtained from the linear plots of pseudo-second order kinetics model. Therefore, the rate-limiting step may be the chemical adsorption mechanism. This suggests that AY25 dye adsorption onto chitin occurred by both internal and external mass transfer mechanisms.⁷ These results also show that the rate constant is high when the initial dye concentration is low. Similar trend has been reported in literature for RB5 dye adsorption on to chitin.²⁹ Also k_2 increases with the increase of chitin dosage for all the initial dye concentrations tested in this study except for the 58 mg/L of dye concentration with 4 g/L of chitin dosage. This may be due to the experimental error or slight change in experimental conditions.

Table 11: Kinetic parameters for AY25 dye adsorption onto chitin. Data are given in different initial dye concentrations and different adsorbent dosages at 23°C and pH=2. Range of particle size of chitin (297-177 μm), Concentration (mg/L), q_e (mg/g), k_1 (min^{-1}), k_2 ($\text{g mg}^{-1} \text{min}^{-1}$).

Initial dye concentration	$q_{e,exp}$	Pseudo-first order			Pseudo-second order		
		$q_{e,cal}$	k_1	R^2	$q_{e,cal}$	k_2	R^2
58 ^a	17.73	0.097	0.002	0.0427	17.67	0.3027	0.9999
58 ^b	13.54	0.124	0.008	0.7734	13.49	1.1362	0.9999
58 ^c	10.85	0.163	0.016	0.7404	10.82	0.6668	0.9999
165 ^a	53.88	1.16	0.031	0.8454	54.35	0.0385	1.0000
165 ^b	35.87	0.434	0.014	0.5338	35.97	0.1137	1.0000
165 ^c	28.82	0.113	0.008	0.6067	28.82	0.5016	1.0000
284 ^a	92.07	17.29	0.040	0.9437	92.94	0.0070	0.9999
284 ^b	69.32	2.354	0.027	0.8829	69.64	0.0277	1.0000
284 ^c	55.58	0.719	0.013	0.5887	55.56	0.0562	0.9999
385 ^a	127.17	65.90	0.045	0.9818	130.72	0.0021	0.9993
385 ^b	98.08	25.55	0.047	0.9656	99.90	0.0049	0.9997
385 ^c	78.64	4.61	0.032	0.8775	79.18	0.0137	0.9999

^{a,b,c} refer to chitin dosages of 3, 4, and 5 g/L respectively.

4.5.3 Intra particle diffusion model

To investigate the internal diffusion mechanism during the adsorption of dye onto chitin, the intra particle diffusion equation was used. It is considered that adsorption is usually controlled by an external film resistance and/or mass transfer is controlled by internal or intra-particle diffusion.¹⁴ The possibility of intra particle diffusion resistance affecting adsorption was explored using Equation 9.

$$q_t = k_p t^{1/2} + C \quad \text{Equation 9}^{14}$$

Where k_p is the intra particle diffusion rate constant ($\text{mg.g}^{-1}.\text{min}^{-1/2}$). It is determined from the linear graph of q_t versus $(\text{time})^{1/2}$.

Values of C provides information about the thickness of the boundary layer: the larger the intercept, the greater the boundary layer effect is. According to this model, a plot of uptake should be linear if intra particle diffusion is involved in the adsorption process. If these lines pass through the origin, then intra particle diffusion is the rate controlling step. When the plots do not pass through the origin, this indicates some degree of boundary layer control. It also indicates that the intra particle diffusion is not the only rate-limiting step, but also other kinetic models may control the rate of adsorption, all of which may be operating simultaneously.¹⁴

In some cases, three linear sections on the plot of q_t vs. $t^{1/2}$ can be identified. That means two or three steps can occur. The first portion represents external surface adsorption or an instantaneous adsorption stage. The second portion is a gradual adsorption stage, where the intra-particle diffusion is the controlling factor. The third portion is a final equilibrium

stage where the intra-particle diffusion starts to decelerate due to extremely low solute concentrations in the solution.¹⁴

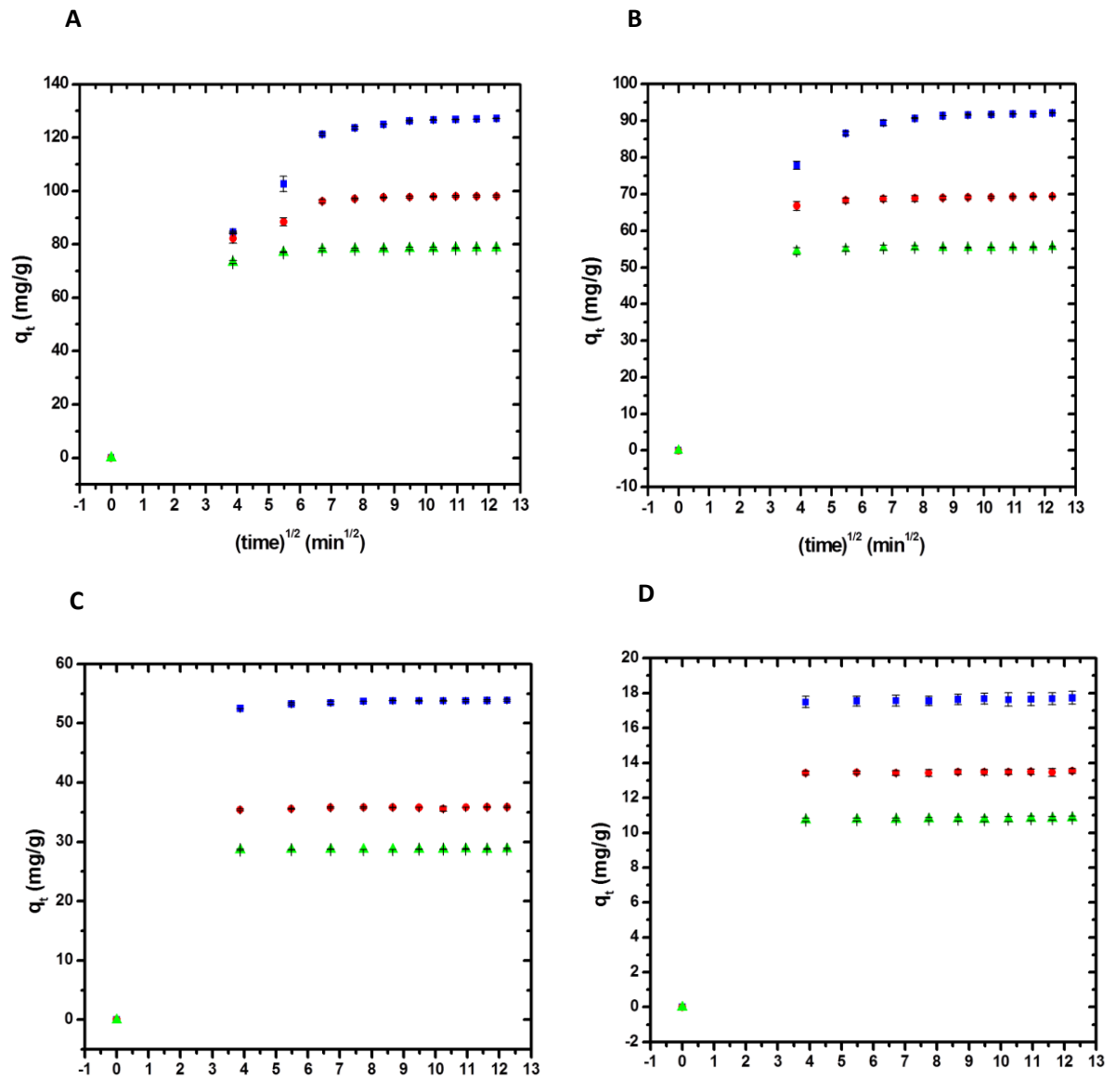


Figure 19: Intra particle diffusion model for AY25 dye adsorption onto chitin. (Weber-Morris plots for different initial dye concentrations and different chitin dosages at 23°C and pH=2. (A) 385 mg/L, (B) 284 mg/L, (C) 165 mg/L, (D) 58 mg/L. Blue, red and green marks represent the chitin dosages of 3, 4 and 5 g/L)

Figure 19 shows the Weber and Morris plots for AY25 dye adsorption onto chitin.

The plots of q_t versus $t^{1/2}$ show multi-linearity. According to Weber and Morris, each portion

represents a distinct mass transfer mechanism.³³ In the AY25 dye adsorption onto chitin, an initial portion relative to the boundary layer diffusion (film diffusion) was observed until 15–20 min. After this time, equilibrium was achieved. Then the mass transfer step in AY25 dye adsorption onto chitin was the film diffusion. This may be occurred due to the presence of a rigid and nonporous surface and low value of surface area of chitin. In addition, the dye molecular size may be higher than average pore radius of chitin, inhibiting the internal diffusion. This can be confirmed using the BET and SEM method, but due to the lack of facility, these techniques were not used in this study.

4.6 Adsorption Isotherms

Adsorption is usually described through isotherms which is important to evaluate the nature of adsorption. Isotherm testing can also aid in the process of choosing the best adsorbent and best dosage for dye removal needs. To optimize the design of an adsorption system, it is important to establish the most appropriate correlation for the equilibrium curves. Various isotherm equations such as Langmuir, Freundlich, Temkin and D-R isotherm models were tested in this study.

In economical view, these isotherms can be used to evaluate whether the chitin will adsorb the dye to an acceptable level and then to estimate the cost of dye removal. It also allow to calculate the adsorptive capacity that is how well chitin will purify the process liquid.

4.6.1 Adsorbent dosage method³¹

This method is used to determine the required chitin dosage, to calculate the adsorptive capacity at certain level of purification, to compare the performance of different adsorbent and to identify the most cost effective adsorbent. This can also be used to determine how dye removal and adsorptive capacity are influenced by process conditions such as pH, temperature, dye concentration etc.

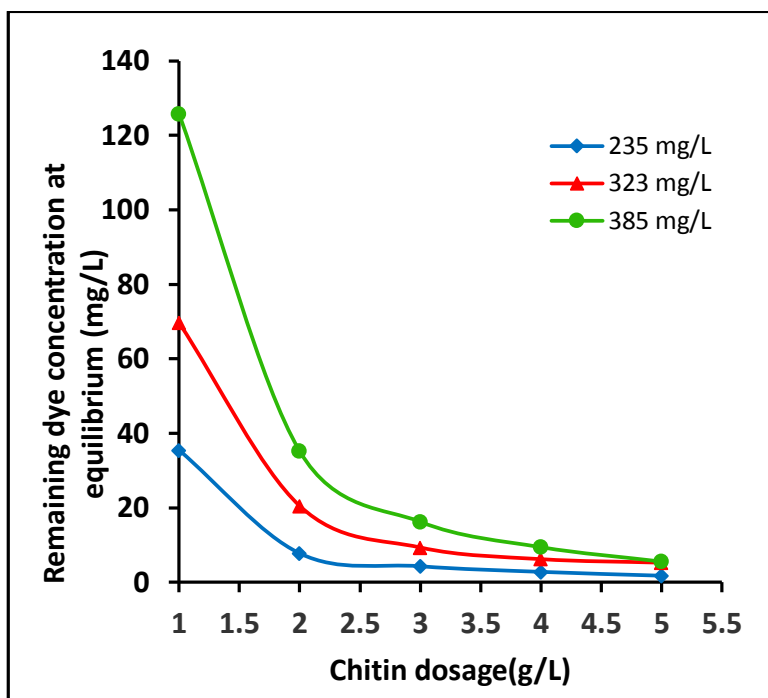


Figure 20: Effect of chitin dosage on equilibrium dye concentration at 23°C and pH=2. Blue, red and green lines indicate the different initial dye concentrations of 235, 323 and 385 mg/L respectively. The figure is representative of three independent, reproducible trials.

Figure 20 shows the effect of chitin dosage on equilibrium dye concentration in three different initial dye concentrations. For initial dye concentration of 235 mg/L, 1.8 g of chitin is sufficient to remove 95% of AY25 dye at 23°C while for higher initial dye concentration of 323 mg/L, 2.2 g of chitin is sufficient to remove 95% of AY25 dye at 23°C. At least 2.7 g of

chitin is needed for 95% dye removal from a solution with 385 mg/L of initial dye concentration.

The main disadvantage of this method is that the curve may be very flat at high level of impurity removal. This makes it difficult to determine the chitin dosage accurately. Therefore, the calculated adsorptive capacity at 95% dye removal for above mentioned initial dye concentrations were quite different each other (Table 12). In such cases, other types of isotherms are used.

Table 12: Adsorptive capacity values at 95% dye removal in three different initial dye concentrations at 23°C according to the adsorbent dosage method

Initial dye concentration mg/L	Adsorptive capacity at 95% dye removal (mg/g)
235	124.03 ± 0.02
323	139.92 ± 0.04
385	137.33 ± 0.17

4.6.2 Langmuir isotherm

The basic assumption of the Langmuir theory is that the adsorption takes place at specific homogeneous sites within the adsorbent. Langmuir equation can be written as follows.

$$\theta = \frac{q_e}{q_{\max}} = \frac{bC_e}{1 + bC_e} \quad \text{Equation 10}^{25}$$

Where, θ = Fractional coverage of the surface
 C_e = Equilibrium concentration of the adsorbate (mg/L)
 q_e = Equilibrium concentration of adsorbate adsorbed per unit amount of adsorbent (mg/g)

q_{\max} = Monolayer saturation capacity of adsorbent (mg/g)

b = Langmuir adsorption constant (L/mg)

The relationship between θ and equilibrium concentration is shown in Figure 21A. It is a gradual positive increase curve that flattens to a constant value. The Langmuir equation shown above can be rearranged as follows.

$$\frac{C_e}{q_e} = \frac{C_e}{q_{\max}} + \frac{1}{bq_{\max}}$$

Equation 11²⁵

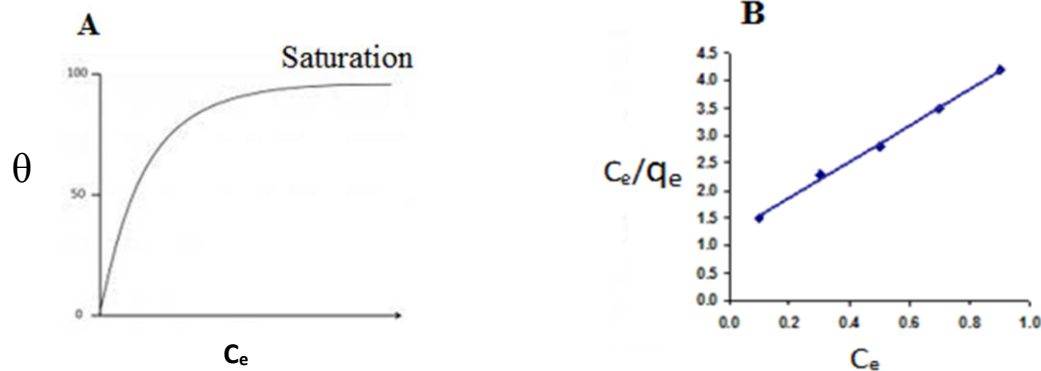


Figure 21: Characteristic shapes of Langmuir saturation curve (A) and linearized plot (B)

A linear plot proves that the system obeys the Langmuir model and the q_{\max} assists in the comparison of adsorption performance. It's a measure of adsorptive capacity.

The essential characteristic of the Langmuir isotherm can be expressed by the dimensionless constant called the equilibrium parameter (Separation factor), R_L , defined by equation 12.

$$R_L = \frac{1}{(1+bC_0)}$$

Equation 12²⁵

Where C_0 is the initial dye concentration (mg L^{-1}).

R_L values indicate the type of isotherm to be irreversible ($R_L=0$), favorable ($0 < R_L < 1$), linear adsorption ($R_L=1$), or unfavorable ($R_L > 1$).²⁵ The R_L values for the adsorption of AY25 dye onto chitin are shown in Table 13.

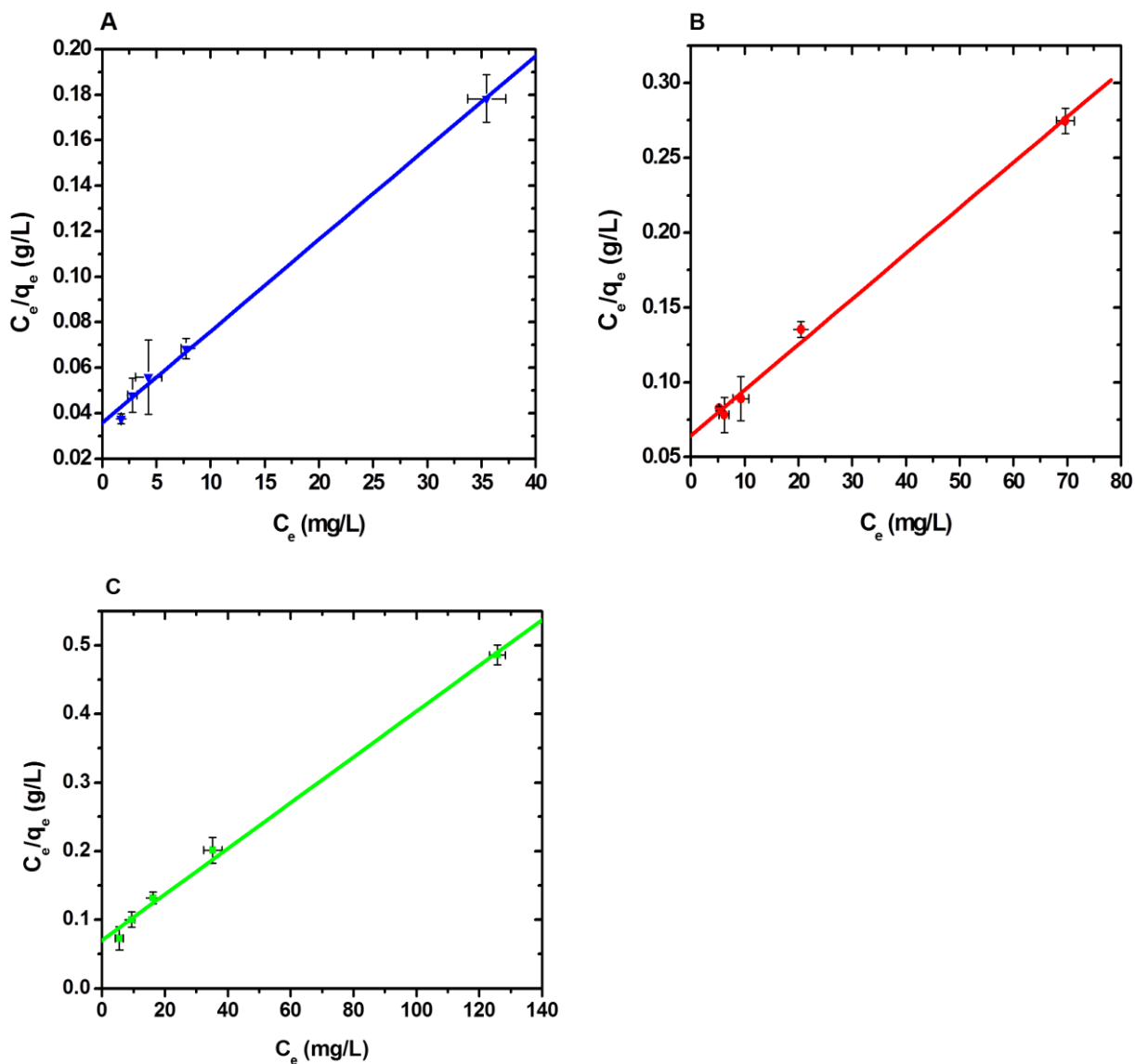


Figure 22: Langmuir adsorption isotherm plots for the AY25 dye adsorption onto chitin. Blue, red and green lines show three different initial dye concentrations, 235 mg/L (A), 323 mg/L (B), 385 mg/L (C) at 23°C, pH=2. Range of particle size of chitin = 297-177 μ m, Amount of chitin (1, 2, 3, 4 and 5 g/L), Volume of dye solution = 100 mL

Table 13: Langmuir adsorption isotherm parameters for AY25 dye adsorption onto chitin at 23°C

Initial dye concentration (mg/L)	R²	q_{max} (mg/g)	b (L/mg)	R_L
235	0.9875	238	0.134	0.031
323	0.9948	333	0.045	0.064
385	0.9951	303	0.045	0.055

According to the R² values, it can be concluded that the experimental data best fit with the Langmuir adsorption model. Also the calculated R_L values indicate that the AY25 dye adsorption onto chitin is favorable at 23°C since they are in between 0 and 1. Since Langmuir model is based on the assumption that adsorption exists up to the formation of a homogeneous monolayer, a tendency to saturate the interaction sites of chitin could be deduced from these results.

4.6.2.1 Basic assumptions of the Langmuir model

This isotherm is based on several assumptions. It is assumed that the energy is same all over the surface and adsorbing sites are homogeneous and equivalent. Adsorbate molecules adsorb at the fixed number of localized sites on the surface and they don't migrate over the surface. Each adsorption site can only accommodate one molecule. There is no interaction between adsorbate molecules on adjacent sites. Adsorption is assumed to occur via monolayer coverage of the adsorbate at the outer layer of the adsorbent even at the maximum adsorption. Therefore this isotherm considers that the energy and enthalpy resulting from adsorption are the same.³⁴

But, these assumptions are not always satisfied with all systems due to the surface roughness, inhomogeneity, multiple site types and interaction of adsorbates adsorbed on to the neighboring sites. Also, the adsorption mechanism is clearly not the same for the first as for the last molecules. Such systems are deviated from Langmuir isotherm model. In such a case a modified form of the Langmuir isotherm, BET isotherm or Freundlich isotherm are considered.¹⁴

4.6.3 Freundlich isotherm

The Freundlich isotherm is used to describe non-ideal adsorption on to heterogeneous surfaces. In other words, it does not consider all sites on the adsorbent surface to be equal. This is the most important multisite adsorption isotherm for rough surfaces. Furthermore, it is assumed that, once the surface is covered, additional adsorbate species can still be accommodated. That is multilayer adsorption is predicted by this model.¹⁴ Freundlich isotherm is given by equation 13. This equation shows that adsorptive capacity (q_e) depends upon the equilibrium concentration of dye remaining. The q_e value will be higher at higher dye concentration.

$$q_e = K C_{eq}^{1/n} \quad \text{Equation 13}^{14}$$

This can be rearranged to a linear form (Equation 14) and makes it easier to determine the adsorptive capacity at the desired level of dye removal.

$$\log q_e = \frac{1}{n} \log C_{eq} + \log K \quad \text{Equation 14}^{14}$$

Where, q_e = Amount of adsorbate adsorbed per unit amount of adsorbent
at equilibrium (mg/g)

C_e = Concentration of adsorbate remaining in liquid at equilibrium (mg/L)

K = Freundlich constant (L/g)

$1/n$ = Heterogeneity factor (adsorption intensity)

K and n are constants at given temperature. K is the adsorption capacity at unit concentration. The $1/n$ values indicate the type of isotherm to be irreversible ($1/n = 0$), favorable ($0 < 1/n < 1$), or unfavorable ($1/n > 1$).⁴ If $n = 1$ then the partition between the two phases are independent of the concentration.³²

4.6.3.1 Advantages of using Freundlich isotherm plots in adsorption studies

Freundlich isotherm can be used to determine whether it is possible to reach a desired purity level with desired adsorbent. It also allow calculation of adsorptive capacity at equilibrium which has a major impact on process economics. It is also used to predict the relative performance of different types of adsorbent and hence the most cost effective chitin. It can also be used to determine how dye removal and adsorptive capacity are influenced by the changes in process conditions such as pH, temperature, dye concentration. The position and slope of the isotherm lines reveal how well adsorbent performs relative to another one. Higher the isotherm line means, higher the adsorptive capacity. Horizontal line means the chitin has good adsorption through a wide range of dye concentration. A nearly vertical isotherm line shows poor adsorptive properties at lower dye concentrations.³²

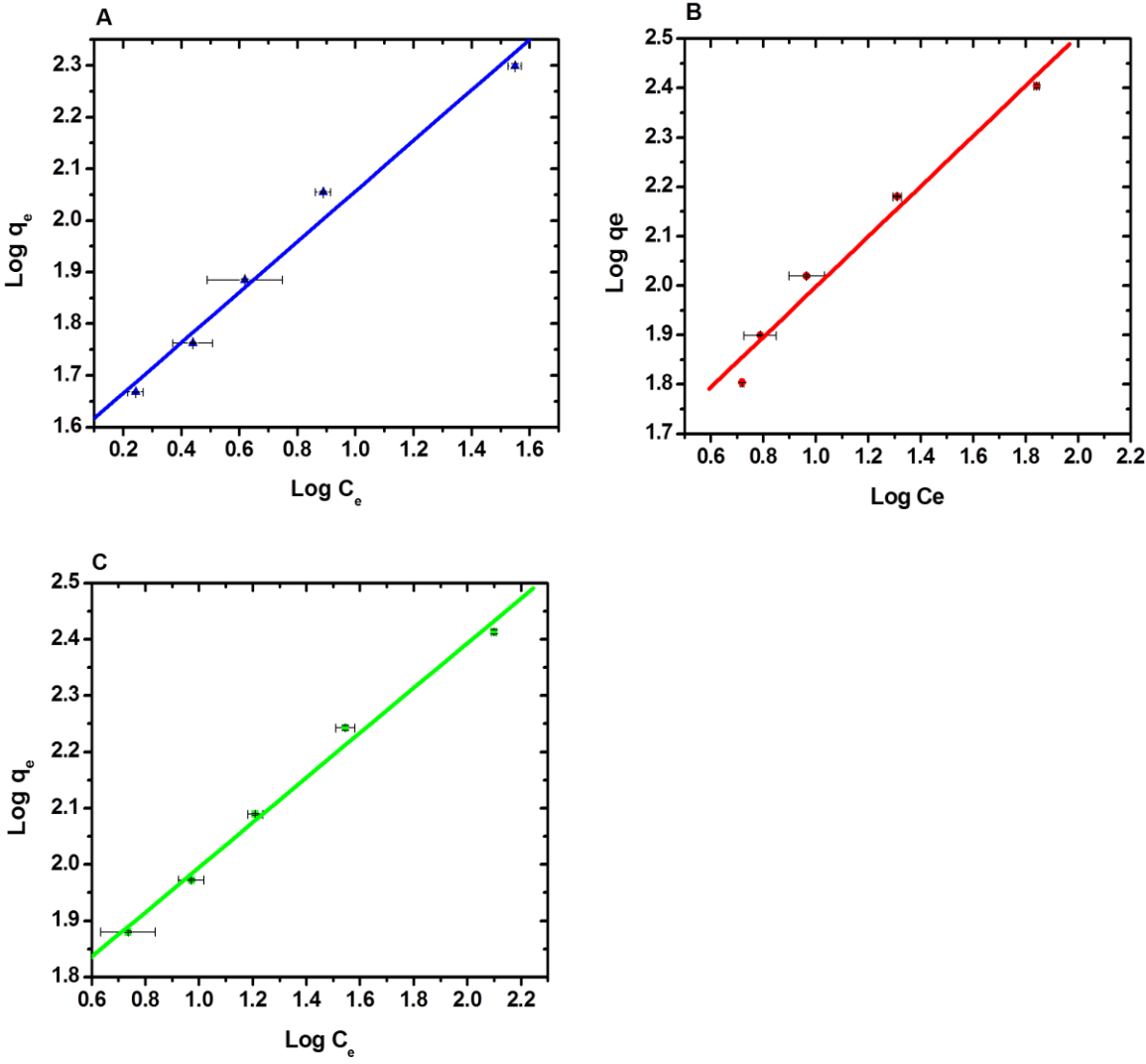


Figure 23: Freundlich adsorption isotherm plots for the AY25 dye adsorption onto chitin. Blue, red and green lines show three different initial dye concentrations, 235 mg/L (A), 323 mg/L (B), 385 mg/L (C) at 23°C, pH=2. Range of particle size of chitin = 297-177 μm , Amount of chitin (1, 2, 3, 4 and 5 g/L), Volume of dye solution = 100 mL

Table 14: Freundlich adsorption isotherm parameters for AY25 dye adsorption onto chitin and adsorptive capacities at 95% dye removal at 23°C

Initial dye concentration (mg/L)	R ²	n	K (Lg ⁻¹)	Adsorptive capacity at 95% dye removal
235	0.9890	1.758	33.84	137
323	0.9716	1.625	22.97	127
385	0.9884	2.384	37.35	129

Results show that the n value for AY25 dye adsorption is above 1 thus the adsorption is favorable. The calculated R² values indicate that the equilibrium data in this study fairly agree with the Freundlich model which presents a better adjustment to chitin with heterogeneous adsorption sites. This is probably because multiple interactions are present in this system where dye could interact with different sites of the adsorbent. Differences of K and adsorptive capacity values in different initial dye concentrations can be attributed as experimental errors and slight change in process conditions.

4.6.4 D-R (Dubinin–Radushkevich) isotherm model

This isotherm is used to determine whether the adsorption is chemical or physical in nature.²² The D-R isotherm equation and its linearized form are given in Equation 15 and 16.

$$q_e = q_D \exp(-\beta_D \varepsilon^2) \quad \text{Equation 15}^{35}$$

$$\ln q_e = \ln q_D - \beta_D \varepsilon^2 \quad \text{Equation 16}^{35}$$

Where, q_e = Adsorption capacity at equilibrium (mol/g)

q_D = Dubinin–Radushkevich monolayer saturation capacity (mol/g)

β_D = Constant related to the mean free energy of adsorption per mole of the adsorbate (mol^2/J^2)

\mathcal{E}^2 = Polanyi potential which is related to equilibrium concentration (J^2/mol^2)

$$\varepsilon = RT \ln(1 + 1/C_e) \quad \text{Equation 17}^{35}$$

Where R is the gas constant (8.314 J/mol.K), T is absolute temperature (K) and C_e is the equilibrium dye concentration.

By plotting $\ln q_e$ versus \mathcal{E}^2 , q_D and β_D can be obtained. The constant β_D gives an idea about the mean free energy, E_{DR} (kJ/mol) of adsorption per mole of the dye when it transfer to the surface of the solid from infinity in the solution. If the adsorbent surface is heterogeneous and homogeneous, subregions are considered and mean free energy value could be calculated using equation 18.^{35, 36}

$$E_{DR} = \frac{1}{\sqrt{2\beta_D}} \quad \text{Equation 18}^{35}$$

This parameter is useful for estimating the type of adsorption interaction. If the sorption process is primarily physical in nature, such as Van der Waals forces, the average free energy is typically in the range of 1–8 kJ/mol. If E_{DR} is between 8 and 16 kJ/mol, the adsorption process is chemisorption via ion exchange.³⁶

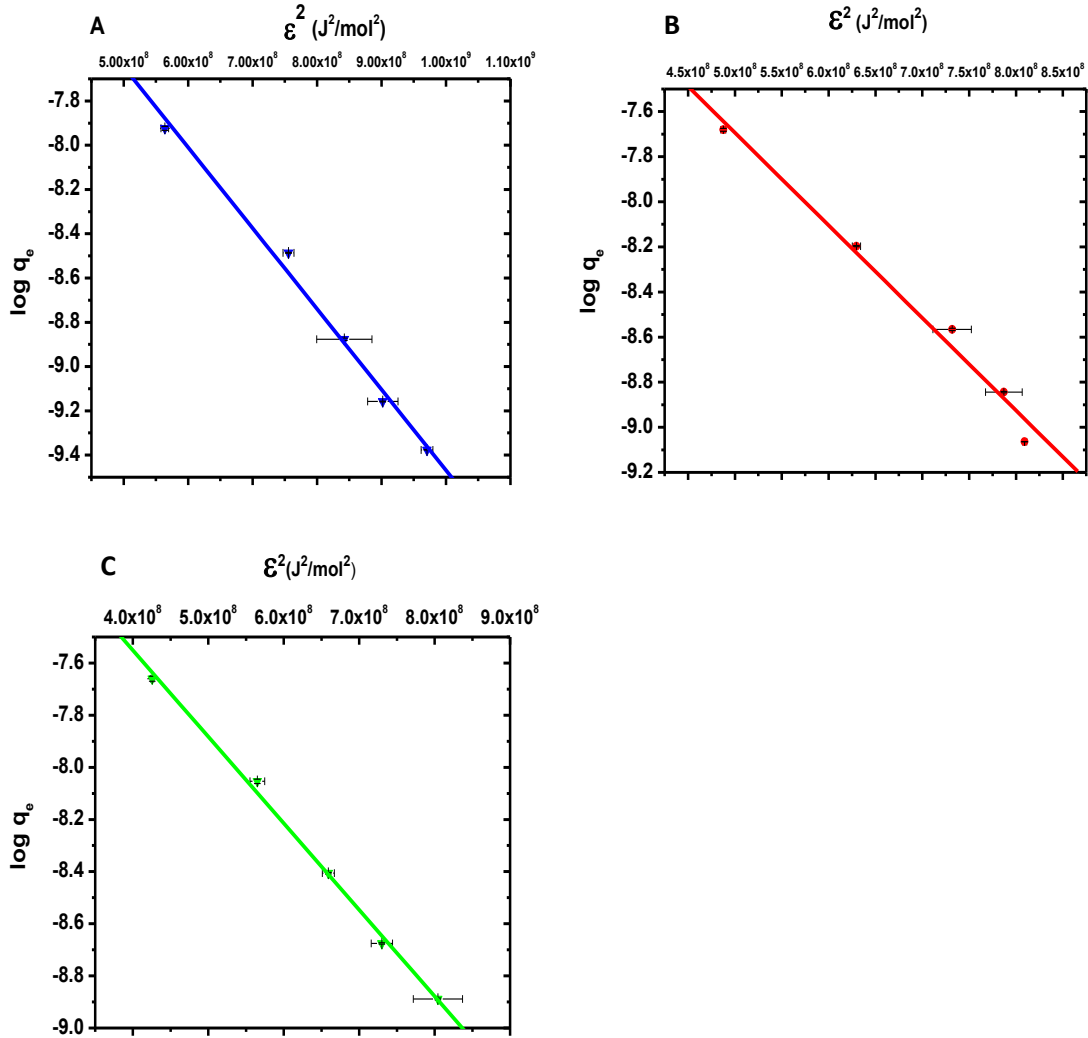


Figure 24: D-R adsorption isotherm plots for the AY25 dye adsorption onto chitin. Blue, red and green lines show three different initial dye concentrations, 235 mg/L (A), 323 mg/L (B), 385 mg/L (C) at 23°C, pH=2. Range of particle size of chitin = 297-177 μm, Amount of chitin (1, 2, 3, 4 and 5 g/L), Volume of dye solution = 100 mL

Table 15: D-R isotherm parameters and mean free energy (E_{DR}) values for AY25 dye adsorption onto chitin at 23°C

Initial dye concentration (mg/L)	q_D (mol/g)	β_D (mol ² /J ²)	R ²	E _{DR} (kJ/mol)
235	0.00398	3.97×10^{-9}	0.9908	11.22
323	0.00546	4.76×10^{-9}	0.9792	10.25
385	0.00202	3.36×10^{-9}	0.9934	12.20

The D-R isotherm parameters are listed in Table 10. All initial dye concentrations of AY25 dye tested show good agreement to D–R isotherm model. The correlation for this isotherm is higher compared to the Freundlich isotherm. For almost all concentrations tested, the mean free energy of adsorption calculated for the interaction is between 10 and 13 kJ/mol, which accounts for charge interactions as the main sorption mechanism (chemisorption) Thus, electrostatic attraction between positively charged chitin and negatively charged dye leads to E_{DR} in the range of 8–16 kJ/mol. This possible nature of adsorption was also proved by the pseudo-second order kinetic model.

4.6.5 Temkin isotherm model

This isotherm is used to determine the interaction between adsorbate and adsorbent. By ignoring the extremely low and higher concentrations of dye, the model assumes that heat of adsorption of all molecules in the layer decreases linearly with surface coverage because of adsorbent-adsorbate interactions.³⁵ Adsorption is characterized by a uniform distribution of binding energies, up to some maximum binding energy.^{4,35} Temkin adsorption isotherm is given in equation 19.

$$q_e = \frac{RT}{b_T} \ln(A_T C_{eq}) \quad \text{Equation 19}^{35}$$

Where, R = Universal gas constant (8.314 J mol⁻¹ K⁻¹)

T = Absolute temperature (K)

A_T = Temkin isotherm equilibrium binding constant (L/mg)

b_T = Temkin isotherm constant related to the heat of adsorption (J/mol)

Equation 19 can be rearranged to test the experimental data. It is given in equation 20.

$$q_e = B \ln A_T + B \ln C_{eq} \quad \text{Equation 20}^{35}$$

$$\text{where, } B = \frac{RT}{b_T}$$

B is a constant related to heat of sorption. A plot of q_e versus $\ln C_{eq}$ enables the determination of the isotherm constants B and A_T from the slope and the intercept respectively. A_T is the equilibrium binding constant corresponding to the maximum binding energy.

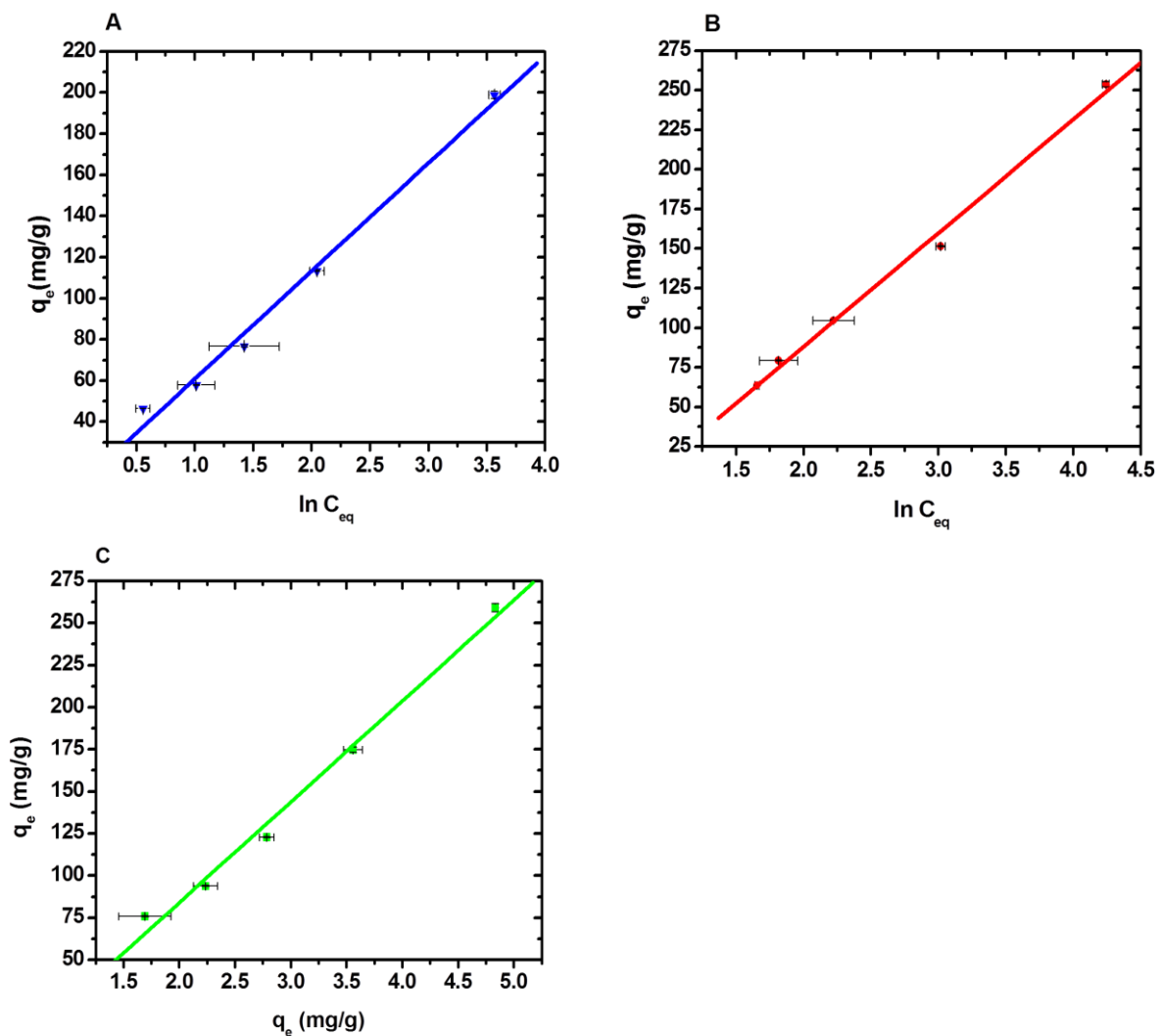


Figure 25: Temkin adsorption isotherm plots for the AY25 dye adsorption onto chitin. Blue, red and green lines show three different initial dye concentrations, 235 mg/L (A), 323 mg/L (B), 385 mg/L (C) at 23°C, pH=2. Range of particle size of chitin = 297-177 μm , Amount of chitin (1, 2, 3, 4 and 5 g/L), Volume of dye solution = 100 mL

Table 16: Temkin adsorption isotherm parameters for AY25 dye adsorption onto chitin at 23°C

Initial dye Concentration (mg/L)	A_T (L/mg)	B	b_T (kJ/mol)	R^2
235	1.878	39.00	0.063	0.9291
323	0.492	67.16	0.037	0.9883
385	0.888	46.14	0.053	0.9467

The calculated coefficient of determination (R^2) shows that the experimental data does not have a good fit with Temkin isotherm (Table 17). Low b_T values indicates that the interaction is neither purely ion-exchange nor physisorption.³⁷

4.7 Adsorption of AY25 dye onto unprocessed chitin

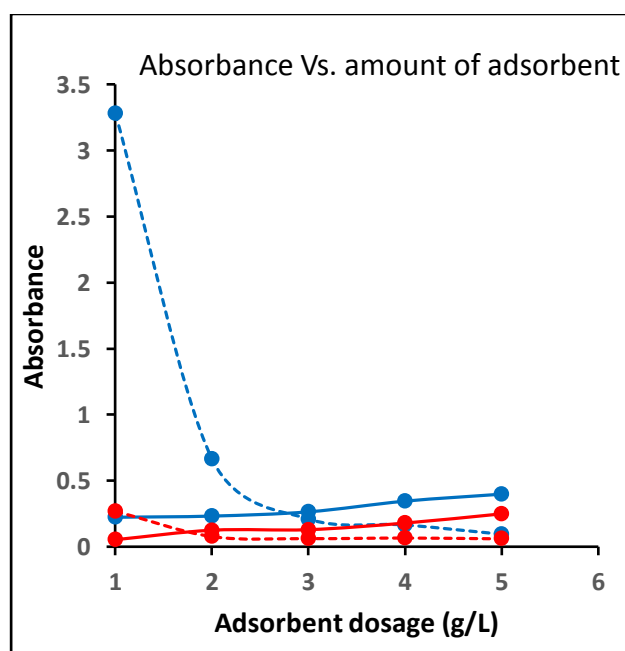


Figure 26: Comparison of dye removal capability of chitin and unprocessed chitin at 23°C. Blue and red colors show the initial dye concentrations of 365 and 140 mg/L. Solid lines indicate the unprocessed chitin while dash lines indicate the purified chitin as adsorbent.

To reduce the process cost, suitability of unprocessed chitin (Crab shell powder) as an adsorbent was also determined by using the batch experiment test in same experimental conditions. It is expected that absorbance decreases with the increase of amount of adsorbent. But in the case of unprocessed chitin, absorbance increased with the increase of adsorbent dosage in both 365 and 140 mg/L of initial dye concentrations tested in this study. This may be due to the release of some pigments in unprocessed chitin during in contact with dye which contribute to the higher absorbance values. None of the isotherm couldn't be produced using unprocessed chitin, meaning that it is not a good adsorbent for dye removal.

4.8 Effect of raw material of chitin

Chitin purified from crab shells and red lobster shells was tested separately to identify the effect of the source of chitin for the dye removal efficiency. Experimental data was tested with Freundlich isotherm. Adsorption capacity at 95% dye removal was calculated to determine the most effective source. Calculated Freundlich isotherm parameters are shown in Table 18.

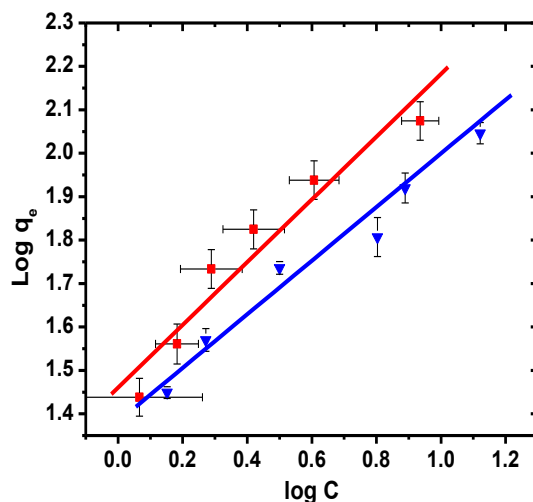


Figure 27: Freundlich adsorption isotherm plots for the AY25 dye adsorption onto chitin. Dye concentration = ~60 mg/L, pH=2, 23°C, Range of particle size = 297-177 μ m, Amount of chitin (1, 2, 3, 4 and 5 g/L), Volume of dye solution = 100 mL, Blue and red lines show the chitin extracted from crab legs and red lobster shells respectively.

Table 17: Freundlich adsorption isotherm parameters for AY25 dye adsorption onto chitin and adsorptive capacities at 95% dye removal at 23°C

Raw material of chitin	Initial dye concentration (mg/L)	R ²	n	K (Lg ⁻¹)	Adsorptive capacity at 95% dye removal	Chitin usage rate (g/L)
Crab	60	0.9639	1.74	24.89	46	1.196
Red lobster	60	0.9143	1.39	28.92	61	0.877

$$\text{Rate of chitin usage} = \frac{\text{Concentration of dye removed}}{\text{Adsorptive capacity}} \quad \text{Equation 21}^{32}$$

As shown in Table 18, adsorptive capacity is higher for chitin extracted from red lobster shells for the initial dye concentration of ~60 mg/L tested at 23°C. Chitin usage can be calculated using Equation 21.³² From the calculated results it is apparent that approximately 36% more crab chitin is required to achieve the same treatment results as obtained with red lobster chitin. These results can be used to determine the most cost effective chitin for certain purification application.

CHAPTER 5

CONCLUSION

Chitin, the proposed adsorbent material in this study, was successfully extracted from waste crab legs with a yield of ~28 %. This indicates that the production of chitin was high (approximately 93%) on the laboratory scale. The FTIR and XRD techniques confirmed that the purified chitin is in its α -form.

Batch treatment test results showed that there is an effect of adsorbent dosage on percentage of dye removal. According to the results, initial dye concentration also played an important role in adsorptive capacity. At low initial dye concentrations, the adsorption of dye onto chitin was very intense and reached equilibrium very quickly. The amount of dye adsorbed onto chitin increases with an increase in the initial dye concentration at a constant amount of adsorbent but the adsorptive capacity was decreased for all the initial dye concentrations. The adsorption of AY25 dye onto chitin was a very fast process, reaching the maximum adsorption capacity (q_e) within 45 minutes with the chitin dosage of at least 0.3 g for all initial dye concentrations tested in this study. On the basis of the data of the present study, one could conclude that the chitin can be effectively used as an adsorbent material for the removal of AY25 dye and it is inexpensive and eco-friendly adsorbent for dye removal.

The typical dye concentration in the dyeing process is 2-3 g/L, and no aggregation/precipitation phenomena are taking place. This happens if the approximate dye concentration is 10 g/L.¹⁷ Given that the initial dye concentrations used in the current study were in the range of 0.05-0.3 g/L, the possibility of dye aggregation/precipitation phenomena, as a way of dye removal, is unlikely. Therefore, the high adsorption capacities presented were only due to the adsorption process.

The kinetic studies of AY25 dye onto chitin was performed and fitted with pseudo-first order, pseudo-second order, and intraparticle diffusion rate mechanisms. Our results indicated that the AY25 dye adsorption can be described best by a pseudo-second order model in a variety of dye concentrations. Therefore, the overall rate of dye adsorption is controlled by adsorption reaction through chemisorption. On the other hand, the intra-particle diffusion is not involved in adsorption process since the data showed multi-linearity. Therefore, AY25 dye adsorption onto chitin is controlled only by film diffusion.

The equilibrium data were analyzed using the Langmuir, Freundlich, D-R and Temkin isotherms. The adsorption data showed good correlation for all isotherm models except for Temkin model. Among them, Langmuir isotherm showed the highest correlation. These results proved that the chitin has both monolayer and heterogeneous adsorption sites. Separation factor (R_L) indicated that this adsorption is favorable. Also from Freundlich isotherm model, the adsorption intensity (n) supports the same conclusion that the process is a favorable adsorption. According to the Freundlich model, the adsorption capacities at 95% dye removal were 137, 127 and 129 mg/g for initial dye concentrations of 235, 323 and 385 mg/L respectively. Based on the D-R model, the mean free energy of adsorption was between 10 and 13 kJ/mol for all concentrations tested which account for the adsorption of AY25 dye onto chitin was via ion-exchange (chemisorption). This possible nature of adsorption was also proved by the pseudo-second order kinetic model.

Unprocessed chitin didn't act as a good adsorbent material. Freundlich isotherm study demonstrated that the rate of dye adsorption onto chitin differed depending on the raw material of chitin. Interestingly, chitin extracted from red lobster shells showed higher adsorptive capacity than that of crab legs.

REFERENCES

1. Dotto, G.L.; Vieira, M.L.G.; Pinto, L. A. Kinetics and Mechanism of Tartrazine Adsorption onto Chitin and Chitosan. *Ind. Eng. Chem. Res.* **2012**, *51*, 6862–6868.
2. Shertate, R.S.; Thorat, P.R. Biotransformation of a Textile AZO Dye Acid Yellow 25 by *Marinobacter Gudaonensis* AY-13. *J. Eng. Com. & App. Sci. (JEC&AS)* **2013**, *2*, 4, 35-45.
3. Kumar, B.A.V.; Varadaraj, M.C.; Tharanathan, R.N. Low Molecular Weight Chitosans - Preparation with the Aid of Pepsin, Characterization, and Its Bactericidal Activity, *Biomacromolecules* **2007**, *8*, 566-572.
4. Santa Cruz Biotechnology Inc. Material Safety Data Sheet 2010.
5. Blackburn, R. Natural Polysaccharides and Their Interactions with Dye Molecules: Applications in Effluent Treatment. *Environ. Sci. Technol.* **2004**, *38*, 4905-4909.
6. <http://www.sigmaaldrich.com/catalog/product/sial/201960?lang=en®ion=US>.
7. Suginta, W.; Khunkaewla, P.; Schulte, A. Electrochemical Biosensor Applications of Polysaccharides Chitin and Chitosan. *Chem. Rev.* **2013**, *113*, 5458–5479.
8. http://www.dfo-mpo.gc.ca/fm-gp/peches-fisheries/reports-rapports/sc-cn_e.pdf
Source: DFO, Statistics Canada, U.S. National Marine Fisheries Service, Bank of Canada.
9. http://www.mdsg.umd.edu/sites/default/files/files/MN15_2.PDF.
10. Kassi, M.R. Various Methods for Determination of the Degree of N-Acetylation of Chitin and Chitosan: A Review *J. Agric. Food Chem.* **2009**, *57*, 1667–1676.
11. F.A. Al Sagheer, F.A.; Al-Sughayer, M.A.; Muslim, S.; Elsabee, M.C. Extraction and characterization of chitin and chitosan from marine sources in Arabian Gulf. *Carbohydrate Polymers* **2009**, *77*, 410–419.
12. Saibaba, N.K.V.; King, P.; Gopinadh. R.; Sreelakshmi, V. Response surface optimization of dye removal by using waste prawn shells. *Int. J. Che. Sci. and App.* **2011**, *2*, 3, 186-193.
13. <http://en.wikipedia.org/wiki/Chitin#mediaviewer/File:Chitin.svg>.
14. Martha Benavente, thesis, 2008, Adsorption of Metallic Ions onto Chitosan: Equilibrium and Kinetic Studies, Royal Institute of Technology, Sweden.

15. G. Akkaya et al. Dyes and Pigments. **2007**, 73,168-177.
16. <http://en.wikipedia.org/wiki/Chitosan>.
17. Kyzas, G.Z.; Kostoglou, M.; Lazaridis, N.K. Relating Interactions of Dye Molecules with Chitosan to Adsorption Kinetic Data. *Langmuir* **2010**, 26(12), 9617–9626.
18. <http://www.rsc.org/chemistryworld/2013/08/chitin-biopolymer-chitosan-podcast.21>.
19. S. Karthikeyan et al. Film and Pore Diffusion Modeling for Adsorption of Reactive Red 2 from Aqueous Solution on to Activated Carbon Prepared from Bio-Diesel Industrial Waste, *E-Journal of Chemistry*, **2010**, 7, 175-184.
20. Ruthven, D. M. “Principles of Adsorption and Adsorption Processes”. *John Wiley & Sons*, New York, **1984**, pp. 29.
21. Kim, M.; Chea, G.; Study on the PV Driven Dehumidifying System with Oyster Shell and Thermoelectric Device. *Journal of the Korean Society of Marine Environment & Safety*, **2012**, 18, 3, 287-293.
22. Ling, S.L.Y.; Yee, C.Y.; Eng, H.S. Removal of cationic dye using deacetylated chitin (chitosan). *J.App.Sci*, **2011**, 11, 8, 1445-1448.
23. Gerente, C., Lee, V. K. C.; Le Cloirec, P.; McKay, G. “Application of Chitosan for the Removal of Metals from Wastewaters by Adsorption – Mechanisms and Models Review”. *Critical Reviews in Env. Sci. & Tech.* **2007**, 37, 41–127.
24. Brunauer, S.; Deming, L.; Deming, W.; Teller, E. J. *Am. Chem. Soc.* **1940**, 62, 1723.
25. Mahmoodi, N.M.; Bagher Hayati, B.; Arami. M. Textile Dye Removal from Single and Ternary Systems Using Date Stones:Kinetic, Isotherm, and Thermodynamic Studies *J. Chem. Eng. Data* **2010**, 55, 4638–4649.
26. Shouman, M.A.; Khedr, S.A.; Attia, A.A.; Basic Dye Adsorption on Low Cost Biopolymer: Kinetic and Equilibrium Studies. *IOSR Journal of Applied Chemistry* **2012**, 2, 4, 27-36.
27. Hu, Q.H.; Qiao, S.Z.; Haghseresht, F; Wilson, M.A.; Lu, G.Q. Adsorption Study for Removal of Basic Red Dye Using Bentonite. *Ind. Eng. Chem. Res.* **2006**, 45, 733-738.
28. G. Annadurai et.al. Adsorption of reactive dye on chitin. *Environmental Monitoring and Assessment* **1999**, 59, 111–119.
29. Filipkowska, U.; Rodziewicz, J.; Sobotka, R. Effect of pH value and adsorbent concentration on the effectiveness of adsorption onto chitin and chitosan. *Progress on Chemistry and Application of Chitin*, **2010**, 15, 79-86.

30. Begum, H.A.; Mondal, A.K.; Muslim, T. Adsorptive Removal of Reactive Black 5 from Aqueous Solution using Chitin Prepared from Shrimp Shells. *Bangladesh Pharmaceutical Journal*. **2012**, *15*, 2, 145-152.
31. Akkaya, G.; Uzun, I.; Gu'zel, F. Kinetics of the adsorption of reactive dyes by chitin. *Dyes and Pigments*. **2007**, *73*, 168-177.
32. <http://www.norit.com/Brochure>: Measuring adsorptive capacity of powered activated carbon.
33. Weber, W. J.; Morris, J. C. Kinetics of Adsorption of Carbon from Solutions. J. Sanit. Eng. Div., *Am. Soc. Civ. Eng.* **1963**, *89*.
34. Wong, Y.C., Szeto, Y.S., Cheung, W.H., McKay, G. Adsorption. **2008**, *14*, 11-20.
35. Dada, A.O.; Olalekan, A.P.; Olatunya, A.M. "Langmuir, Freundlich, Temkin and Dubinin–Radushkevich Isotherms Studies of Equilibrium Sorption of Zn²⁺ onto Phosphoric Acid Modified Rice Husk. *IOSR J. App. Che. (IOSR-JAC)*, **2012**, *3*, 1, 38-45.
36. Copello, G.J.; Mebert, A.M.; Raineri, M.; Pesentia, M.P.; Diaza, L.E. Removal of dyes from water using chitosan hydrogel/SiO₂ and chitin hydrogel/SiO₂ hybrid materials obtained by the sol–gel method. *J. Hazardous Materials*, **2011**, *186*, 932–939.
37. Kiran Munir et.al. *Pak.J. Bot.* **2010**, *42*, 1, 593-604.